

## ELECTROPHYSIOLOGICAL ANALYSIS OF POTASSIUM AND SODIUM MOVEMENTS IN CRUSTACEAN NERVOUS SYSTEM

By N. JOAN ABBOTT,\* R. B. MORETON† AND Y. PICHON

*Laboratoire de Neurobiologie Cellulaire de C.N.R.S.,  
Gif-sur-Yvette 91190, France*

(Received 20 December 1974)

### SUMMARY

1. An electrophysiological method was used to estimate the half-times for sodium and potassium entry to, and efflux from, the extra-axonal space in peripheral nerve and central nervous connectives of two species of crustacean. Results from crab (marine) and crayfish (fresh water) were qualitatively similar.

2. Peripheral nerve showed no evidence for diffusion barriers, potassium entry and efflux being rapid, and proceeding at comparable rates.

3. In connective, potassium entry was extremely slow, with a half-time greater than 100 min, while potassium efflux was relatively rapid ( $T_{\frac{1}{2}} = 6$  min). Sodium movements were less restricted, but sodium entry was more rapid than sodium efflux.

4. The potassium experiments were compared with the behaviour of a theoretical model system. Evidence is presented for diffusional restriction to potassium at the connective perineurial layer. The mechanism of restriction may involve changes in permeability or activation of an ion pump in the perineurial layer.

5. The physiological significance of these findings is discussed.

### INTRODUCTION

In studies in the cockroach (Treherne, Lane, Moreton & Pichon, 1970; Pichon & Treherne, 1970; Pichon, Moreton & Treherne, 1971) it was observed that large rapid potential changes could be recorded in intact central nervous connectives, following an elevation of potassium concentration in the bathing medium. As intracellularly recorded action potentials showed no equivalent reduction in amplitude, it was suggested that the apparent depolarization ('extraneuronal potential') was not due to depolarization of axon membranes. It was suggested that the extraneuronal potentials could result from depolarization of the outward-facing membrane of the perineurium, the peripheral layer of connective glial cells. A small but finite permeability of perineurial junctions was also proposed: the most likely explanation for marked resistance of the action potential to a high bathing potassium concentration

\* Department of Physiology, King's College, Strand, London WC2R 2LS.

† ARC Unit of Invertebrate Chemistry and Physiology, Department of Zoology, Downing Street, Cambridge.

is that a barrier of restricted permeability is present in the diffusion path. Electron-microscopical study showed that lanthanum and microperoxidase entry was blocked by tight junctions between perineurial cells (Lane & Treherne, 1972).

These observations are of considerable comparative interest among blood-brain barrier studies, for extraneuronal potentials should be observable in neural structures wherever a change in ionic composition of the bathing medium results in a change in the potential difference across a peripheral cellular layer. Interest in the crustacean blood-nerve and blood-brain interface has been less marked than in the equivalent insect systems. However, early studies by Prosser (1940*a*, *b*, 1943) and Roeder (1941) suggested that raised or lowered potassium concentration in the medium bathing isolated crayfish ganglia and connectives rapidly affected axonal conduction and synaptic discharge. There was some indication that undissected preparations were more resistant to alterations in the bathing potassium concentration (Prosser, 1940*a*). Recent studies of the blood-brain interface of crustacean intraganglionic vessels (Abbott, 1970, 1971*b*, 1972; Shivers, 1970; Kristensson, Strömberg, Elofsson & Olsson, 1972) suggest that diffusional restriction at this interface, if present, may be slight.

On the other hand, the superficial layers of crustacean ganglia and connectives resemble those of insects, with a thick neural lamella (collagen and mucopolysaccharide) and distinct underlying glial perineurium (Abbott, 1971*a*; Lane & Abbott, 1975). In the crayfish connective, the lateral membranes of the perineurial cells are apposed in such a way that the extracellular cleft is narrow and tortuous, with junctional complexes which appear to be mainly gap junctions, with occasional punctate tight junctions (Fig. 1*a*) (Lane & Abbott, 1975). It is likely that, as in the insect, the perineurium limits considerably the access of ions and molecules, effectively restricting the pathway for exchange between the blood and the central nervous system to that provided by the walls of intraganglionic blood vessels. The functional significance of such a specialization is open to conjecture, and will be discussed below.

The peripheral nerve-blood interface has received little attention, but observations in Crustacea (Keynes & Lewis, 1951; Baker, 1965*a*, *b*; Evans, 1973) suggest that the interstitial space of nerve is readily accessible to small ions and molecules from the bathing medium. Major branches of insect peripheral nerve possess a peri-

---

Fig. 1. Summary diagram of electron-microscopical findings, crayfish nervous system (Lane & Abbott, 1975).

(*a*) *Connective*. The neural lamella (*nl*), composed of collagen-like fibrils embedded in an amorphous matrix, is unlikely to restrict diffusion (cf. Lane & Treherne, 1970). The perineurium (*pn*) is an extensive layer of densely staining glial cells at the blood-connective interface, coupled by gap junctions (large arrows) and occasional zonulae occludentes (small arrows). An intermediate layer of loosely organized glia (*g*) overlies the axon layer, axons themselves (*a*, *ga*) being closely invested by deeper glia (Schwann cells). Extracellular spaces (*e*<sub>1</sub>) in the outer layers frequently contain deposits of collagen, while the extensive extracellular space deeper within the connective (*e*<sub>2</sub>) contains a flocculent material alternating with basal lamina-like strands or sheets (extracellular material omitted from the diagrams for clarity). The extracellular path to the surface of the giant axon (*ga*) may be extremely tortuous, with a path length maximally 500  $\mu$ m.

(*b*) *Peripheral nerve*. The perineurium (*pn*) is reduced to one or a few layers of loosely wrapped glia, with no junctional specializations. Path length to large axons (*a*) may be a few  $\mu$ m to 500  $\mu$ m.

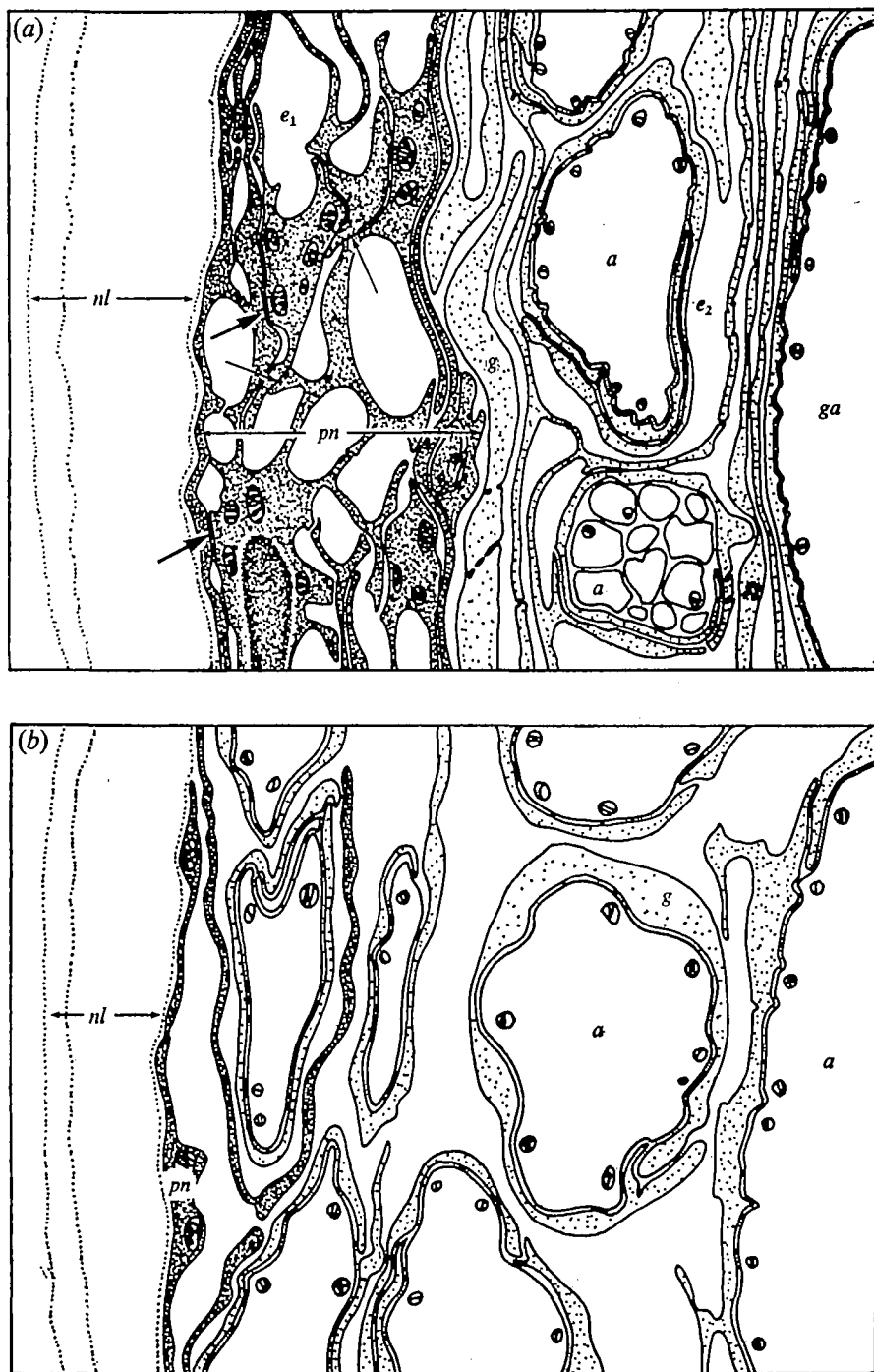


Fig. 1(a) and (b). For legend see opposite.

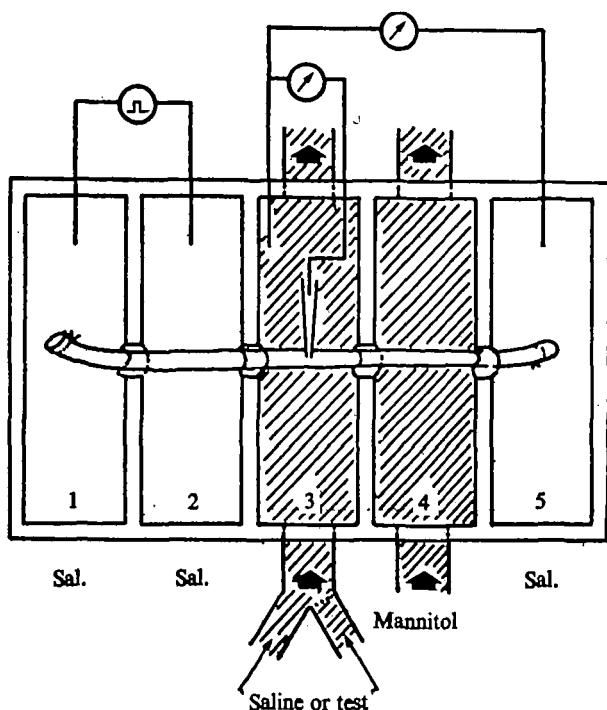


Fig. 2. Perspex chamber, showing preparation and electrode positions. Channels 1, 2 and 5 contain saline; 3, flowing saline or test; 4, flowing mannitol.

neurium tight to lanthanum (Lane & Treherne, 1973), but crustacean nerve has no equivalently organized structure, and the layer(s) of glia that loosely ensheath the axon bundles do not possess junctional complexes (Fig. 1*b*) (Lane & Abbott, 1975).

It thus appeared interesting to compare the characteristics of any potentials measurable across crustacean blood-brain and blood-nerve interfaces with those of insects, both to discover whether the superficial layer might act as an appreciable barrier in Crustacea, and, in the case of differences between the two groups, as an aid to further understanding of the insect system.

A preliminary account of this work has been published (Abbott & Pichon, 1973).

#### MATERIALS AND METHODS

Shore crabs (*Carcinus maenas* L.), carapace width averaging 6 cm, were obtained from the marine laboratory at Roscoff, France, and kept in sea water and damp seaweed in a cold room for up to 5 weeks. Animals were brought gradually to room temperature before use. Leg nerves and circumoesophageal connectives were used. Ringer (Pantin, 1946) had the following composition (mM):  $\text{Na}^+$  494,  $\text{K}^+$  11.3,  $\text{Ca}^{2+}$  9.4,  $\text{Mg}^{2+}$  18.3,  $\text{Cl}^-$  530,  $\text{SO}_4^{2-}$  15.3, buffered to pH 7.5 with 10 mM Tris. Isosmotic mannitol solution contained 200.2 g/l mannitol. Isotonic KCl contained 550 mM-KCl. Where other elevated  $\text{K}^+$  levels were used,  $\text{Mg}^{2+}$  and  $\text{Ca}^{2+}$  concentra-

tions were kept constant, and  $\text{Na}^+$  reduced proportionately.  $\text{Na}^+$ -free solutions were made by substituting Tris for Na.

American crayfish (*Procambarus clarkii*) were flown from the U.S.A. and kept in freshwater tanks. Claw and leg nerves and circumoesophageal connectives were used. Modified Van Harreveld (1936) saline had the following composition (mM):  $\text{Na}^+$  195,  $\text{K}^+$  5.4,  $\text{Ca}^{2+}$  13.5,  $\text{Mg}^{2+}$  2.6,  $\text{Cl}^-$  229.5, buffered to pH 7.5 with 10 mM Tris. Isosmotic mannitol solution contained 83.63 g/l mannitol. Isotonic KCl solution contained 229.5 mM-KCl. Modified  $\text{K}^+$  and  $\text{Na}^+$  salines were devised as before.

Nerves and connectives were dissected under saline, and mounted in a perspex chamber (Fig. 2) with petroleum jelly seals between compartments. Unless otherwise stated, single intact connectives were used, without further dissection. In experiments where connectives were desheathed, the complex of perineurium and neural lamella was removed with sharpened steel needles. Stimuli could be applied between compartments 1 and 2, and extracellular potential changes recorded across the flowing mannitol compartment between 3 and 5. Mannitol was used, rather than sucrose as in the standard 'sucrose gap' chamber (Stämpfli, 1954), because of negligible decomposition and ion contamination.

Electrical stimuli were delivered from Tektronix waveform and pulse generators 162 and 161, via a Grass photoelectric stimulus isolator (PSIU 6B) to Ag/AgCl electrodes. Potentials were recorded from compartment 5 connected by a KCl-agar bridge and Ag/AgCl electrode to a high impedance amplifier. The indifferent electrode made contact with the central compartment (3: flowing saline or test solution) via a second KCl-agar bridge. In some experiments on connectives, glass microelectrodes were used to impale giant axons in the central compartment, the preparation being supported on a transparent Elastomere block (Rhône-Poulenc, Paris). Microelectrodes contained 3 M-KCl, and were connected to a second high impedance amplifier. Potentials were recorded on Tektronix oscilloscopes (565 and 564B storage), photographed on Nihon-Kohden or Polaroid cameras. D.c. potentials were continuously recorded on a Sefram 2-channel pen recorder. Compartments 3 and 4 of the chamber were perfused by gravity-feed, and rapid changes of solution in the central channel achieved with a 3-way tap.

#### THEORETICAL ANALYSIS OF A MODEL SYSTEM

In an attempt to achieve a fuller understanding of the electrical behaviour of intact connectives, a theoretical analysis was made of a simple model system. This consisted of a discrete peripheral diffusion barrier, in series with a long channel leading to the giant axon. The peripheral barrier was taken as of the 'constant-field' type (Goldman, 1943), and diffusion in the channel was considered to occur through a uniform medium. This system is very similar to that proposed for the cockroach central nervous connective by Pichon *et al.* (1971): the equations used were the same, and are not given here in full. They were used to calculate the time courses of the peripheral and axonal membrane potentials, following step-changes in external potassium concentration between 'normal' (5.5 mM) and 'isotonic KCl' (230 mM, crayfish concentrations)

For simplicity, the peripheral barrier was taken as a potassium channel in parallel with a non-specific leak. The potential difference across it is then given by

$$\exp \frac{FV}{RT} = \frac{[K_o^+] + A}{[K_i^+] + A}, \quad (1)$$

where  $[K_o^+]$  and  $[K_i^+]$  are potassium concentrations and  $A$  is a constant, representing the amount of leakage of other ions (cf. equation (1) of Pichon *et al.* 1971).  $R$ ,  $T$  and  $F$  have their usual meanings. The data of Fig. 16, plotted in this form, fall approximately on a straight line (Fig. 16, inset), suggesting that equation (2) is a fair representation, at least at concentrations above 20 mM. The value of  $A$  is obtained from the intercept of the line, and is between 10 and 30 mM in different preparations.

The flux of potassium ions across the barrier is then given by

$$\begin{aligned} M_K &= \frac{FV}{RT} P_K \frac{[K_o^+] - [K_i^+] \exp(FV/RT)}{1 - \exp(FV/RT)} \\ &= \frac{FV}{RT} AP_K, \end{aligned} \quad (2)$$

where  $P_K$  is the potassium permeability.

Changes in axonal membrane potential were calculated from the potassium concentration by extrapolating the curve obtained by Dalton (1959) from desheathed crayfish axons. It was found that this curve could be fitted closely by the empirical relation

$$\exp(V/26.9) = \frac{[K^+] + 3.37}{8.86}, \quad (3)$$

where  $V$  is the change in membrane potential in mV, and  $[K^+]$  is the extra-axonal potassium concentration in mM.

Analytical solution of the diffusion equation with the boundary condition expressed by equations (1) and (2) is not possible. The method of numerical analysis is therefore used (cf. Pichon *et al.* 1971). This allows two further sophistications to be introduced. Firstly, step-changes in external concentration can be replaced by an exponential approach to each new level, to allow for mixing in the experimental bath, and the effects of unstirred layers, which become significant in the case of the rapidly developing extraneuronal potentials. The appropriate exponential time-constant was estimated from the experimental rate of development of extraneuronal potentials to be about 6 sec.

Secondly, the effect can be investigated of a return to normal potassium concentration after a pulse of high potassium, during which the system does not fully equilibrate to the higher concentration. This can be done because, at each stage in the calculation, the calculator always carries a complete model of the concentration profile, which is particularly useful in the study of shorter pulses.

Three major parameters remain to be considered: the potassium permeability,  $P_K$ , of the peripheral barrier, the length of the diffusion channel separating it from the extra-axonal space and the effective diffusivity of potassium ions along the channel. The length of the channel, which is composed of extracellular path and

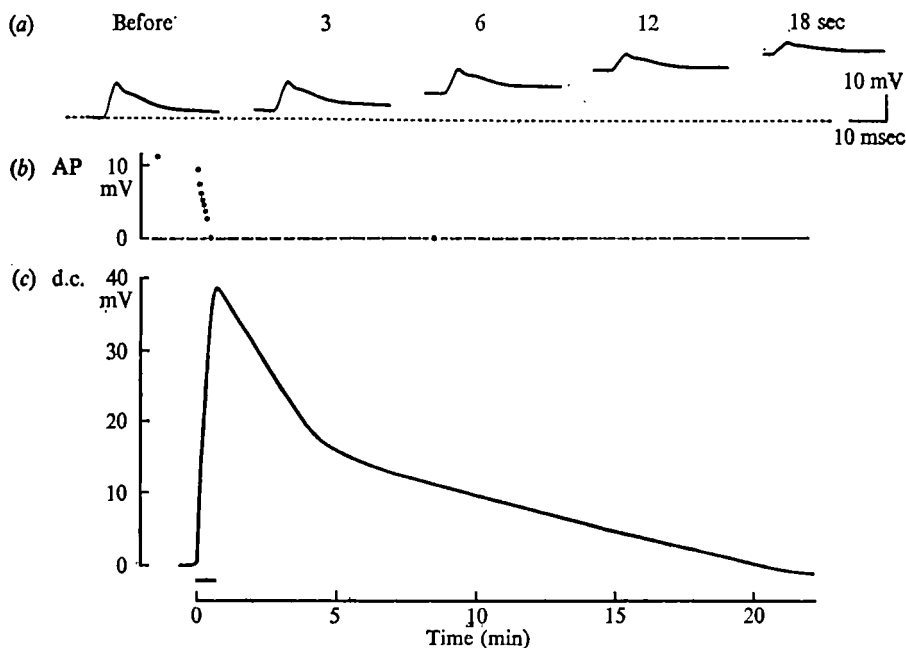


Fig. 3. Crab nerve. Effect of 45 sec isotonic KCl exposure, indicated by horizontal bar. Sucrose gap recording. (a) Compound action potential. (b) Variation of action potential (AP) and (c) d.c. potential (*dc*) with time. In this and subsequent figures, depolarization is shown as an upwards deflection in the d.c. trace.

mesaxon spiral, appears to have a maximum of about  $500\ \mu\text{m}$  (Lane & Abbott, 1975). This figure is not incompatible with potassium half-times in desheathed connectives (Table 1). It turns out to be necessary to assume some degree of restriction to diffusion in the channel; the diffusivity and barrier permeability were therefore treated as two arbitrary constants.

Calculations were performed on a Hewlett-Packard 9810A Desk Calculator and X-Y Plotter.

## RESULTS

Preliminary studies suggested that crab (*Carcinus*) and crayfish (*Procambarus*) preparations behaved in a qualitatively similar manner. Examples from both species will be presented.

### Peripheral nerve

Fig. 3 illustrates the electrical response of crab nerve following exposure to an isotonic (Na-free) KCl solution, recorded with sucrose gap.\* Fig. 3(c) shows a fairly rapid d.c. potential change, an apparent depolarization, while Fig. 3(a) shows a corresponding reduction in height of the compound action potential, plotted against time in Fig. 3(b). The recovery phase of the d.c. potential change is markedly slower than the depolarization phase.

\* In this study, the effects of replacing normal saline by isotonic KCl are interpreted as the effects of high potassium ( $\text{K}^+$  depolarization), assuming that the contribution of  $\text{Na}^+$  ions to resting potentials is negligible.

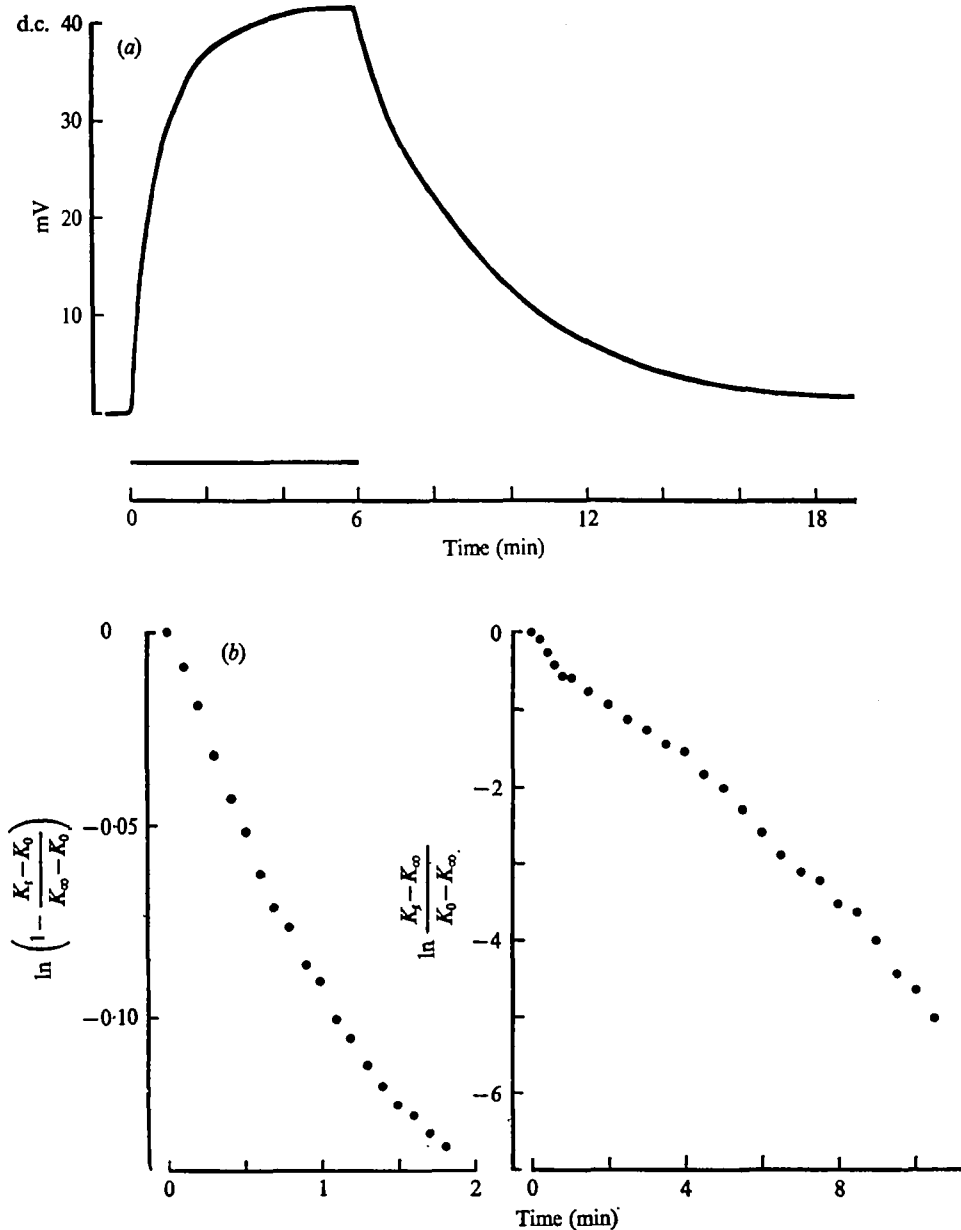


Fig. 4. Crab nerve. (a) Effect of 6 min isotonic KCl on d.c. potential, sucrose gap. (b) Time course of  $[K^+]$  changes at the giant axon surface, expressed as  $\ln [1 - (K_t - K_0)/(K_\infty - K_0)]$  (entry) and  $\ln [(K_t - K_\infty)/(K_0 - K_\infty)]$  (efflux), calculated from (a).  $K_t = [K^+]$  at time  $t$ .  $K_0 = [K^+]$  at time zero, and  $K_\infty = [K^+]$  at equilibrium, assumed to equal potassium concentrations in the bathing medium, before and after the step-change in concentration at time zero.



Table 1. *Half-times ( $T_{\frac{1}{2}}$ ) for  $K^+$  and  $Na^+$  movements between bathing medium and extra-axonal space in different preparations*

Species	Tissue	Ion	Direction of movement	Method	Half time ( $T_{\frac{1}{2}}$ )		
					n	Mean	S.E.
Crayfish	Intact connective	$K^+$	Entry	Regression line, Fig. 14	113	142.53	9.59
			Entry	Reconstruction, Figs. 10(d), 12	1	198.97	—
			Entry	Reconstruction, Fig. 10(d-f)	3	193.51	15.13
			Efflux	Efflux data from experiments used in Fig. 14 for uptake	113	5.99	0.41
			Efflux	Figs. 10(d), 12	1	9.06	—
			Efflux	Fig. 10(d-f)	3	8.74	0.90
	Desheathed connective	$K^+$	Entry	Fig. 15	1	13.08	—
			Efflux	Fig. 15	1	2.45	—
	Peripheral nerve	$K^+$	Entry	Pooled data, e.g. Fig. 15	6	1.85	0.35
			Efflux	Pooled data, e.g. Fig. 15	6	1.16	0.09
Crab	Intact connective	$Na^+$	Efflux	Pooled data, e.g. Fig. 17	3	9.28	2.97
			Entry	Pooled data, e.g. Fig. 17	3	2.91	0.88
	Peripheral nerve	$K^+$	Entry	Regression line, expts. comparable to Fig. 14, crayfish	16	62.60	4.90
			Efflux	Efflux data from same experiments	18	2.60	0.41
			Entry	Pooled data, e.g. Figs. 3, 4	9	2.96	0.51
			Efflux	Pooled data, e.g. Figs. 3, 4	9	1.91	0.15

Longer exposure to KCl (Fig. 4a) results in the apparent depolarization reaching a plateau, with again a slower recovery phase when saline is replaced. These observations are compatible with a direct effect of the elevated potassium concentration in the bathing medium upon the axons; diffusion of  $K^+$  into the nerve interstitial space causes progressive depolarization of axon membranes, resulting in the observed d.c. potential change and eventual action potential block.

In experiments on connective it was shown that the sucrose gap technique reflects axon membrane potential with only a few per cent attenuation. Assuming that the d.c. potential recorded in peripheral nerve is also a measure of axon membrane potential, and with knowledge of the relation between steady state membrane potential and bathing  $[K^+]$ , the time course of  $[K^+]$  change at the surface of the axon can be calculated. Dalton (1958) has investigated the dependence of membrane potential on external  $[K^+]$  in the lobster *Homarus americanus*, and it is likely that a closely similar relation holds for *Carcinus*, with comparable haemolymph composition. Using the lobster figures, the  $[K^+]$  in the fluid bathing the axon membrane has been calculated for the KCl exposure shown in Fig. 4(a). The results are plotted in Fig. 4(b) and show clearly that  $[K^+]$  changes approximately exponentially with time. Mean half-times for  $K^+$  entry to and efflux from the extra-axonal space in crab nerve were 2.96 and 1.91 min respectively (Table 1).

Comparable results are obtained with crayfish claw and leg nerve. Using Dalton's figures for the dependence of the membrane potential on bathing  $[K^+]$  in crayfish

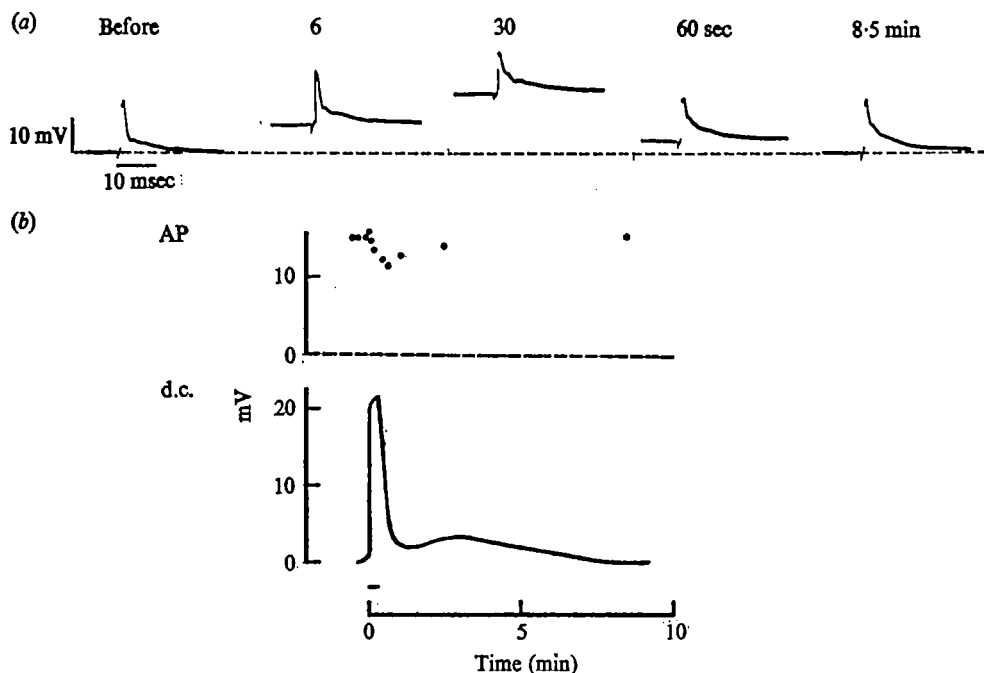


Fig. 5. Crab connective; 20 sec isotonic KCl, sucrose gap. (a) Compound action potential. (b) Variation of AP and d.c. potential with time. Note that the magnitude of the AP is little affected, in spite of large changes in d.c. potential.

(1959), the interstitial  $[K^+]$  can again be calculated. Mean half-times for  $K^+$  entry and efflux in crayfish nerve were 1.85 and 1.16 min respectively (Table 1).

#### Connective

When crab connective is exposed to isotonic KCl, an apparent depolarization and repolarization can again be recorded (Figs. 5, 6). However, the depolarization proceeds more rapidly than in peripheral nerve, and the repolarization phase can generally be seen to contain at least two components – an initial fast phase and a later slow phase. The change in height of the extracellularly recorded action potential does *not* parallel the d.c. potential change, and the height of the action potential may even rise during the depolarization phase of the d.c. potential change. Comparison of the time course for decay of d.c. potential and action potential in peripheral nerve and connective (Fig. 7) clearly shows that the two structures behave in qualitatively different ways.

In records obtained from intracellular microelectrodes within crayfish connective giant axons, this apparently paradoxical situation is even more marked, with action potential amplitude clearly unrelated to the extent of the d.c. apparent depolarization (Fig. 8). During longer exposures to KCl (Fig. 9) the d.c. potential gradually declines after an initial maximum, and the recovery phase shows the two components characteristic of connective. The lack of correlation between the amplitude of the action potential and the d.c. potential change suggests that the latter is not solely due to depolarization at the axon membrane.

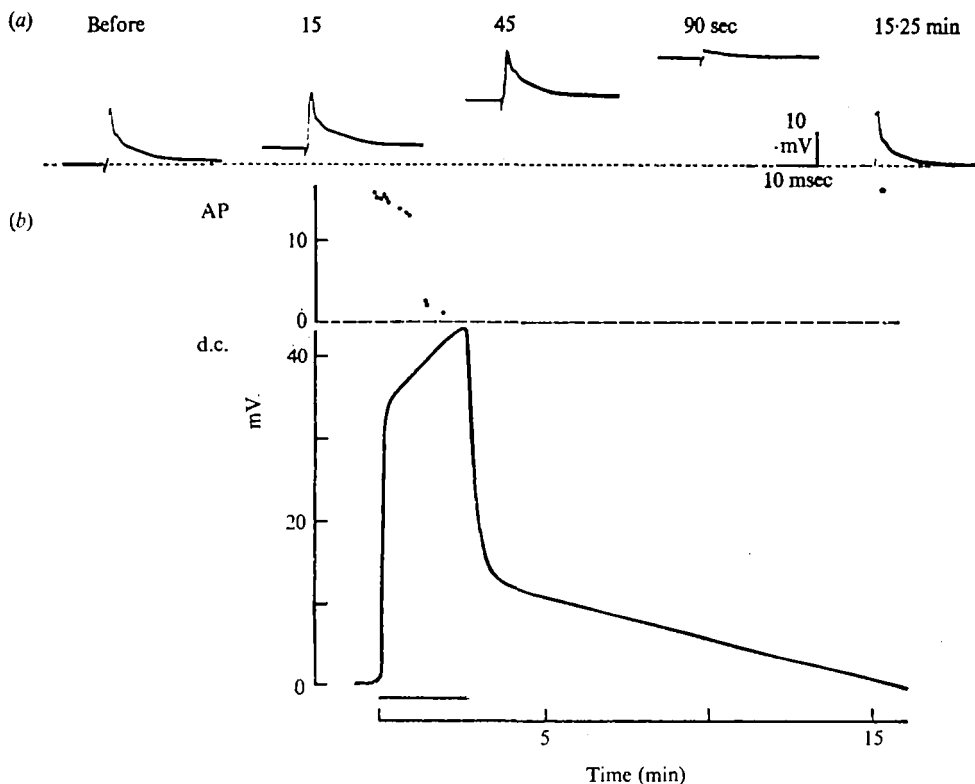


Fig. 6. Crab connective; 2.75 min isotonic KCl, sucrose gap. (a) and (b) as in Fig. 5. The AP shows little change initially, in spite of rapid depolarization of the d.c. trace.

In an attempt to localize the site of origin of the d.c. potential, the response to KCl exposure was recorded simultaneously by the extracellular sucrose gap technique, and by a microelectrode either within a giant axon, or in an extracellular position within the crayfish connective (Fig. 10). A small (5 %) correction for the attenuation of the sucrose gap d.c. record (solid line in Fig. 10a, b) renders it superimposable on the intracellular microelectrode trace (dashes + dots).

When the microelectrode is withdrawn into an extracellular position within the connective (arrow, Fig. 10), a difference from the sucrose gap record is apparent for short KCl exposures (10c), and even more marked for longer exposures (10d-f). While the early fast depolarization phase is similar, subsequent potential changes are not. Of particular interest is the steady level of potential recorded by the extracellular microelectrode after the initial rapid transient (Fig. 10d, e), while the sucrose gap record shows a gradual depolarization. The repolarization time course, which is rapid with the microelectrode, is two-phase in the sucrose gap trace.

#### *Model for d.c. potential changes*

As the d.c. potential changes we are monitoring are obviously quite complex, it is useful to introduce a model of the system. Fig. 11(a), (c) shows the electrode positions used (sucrose gap and extracellular microelectrode) and the d.c. records obtained in the preparation shown in Fig. 10(d). Fig. 11(b) shows the record that would

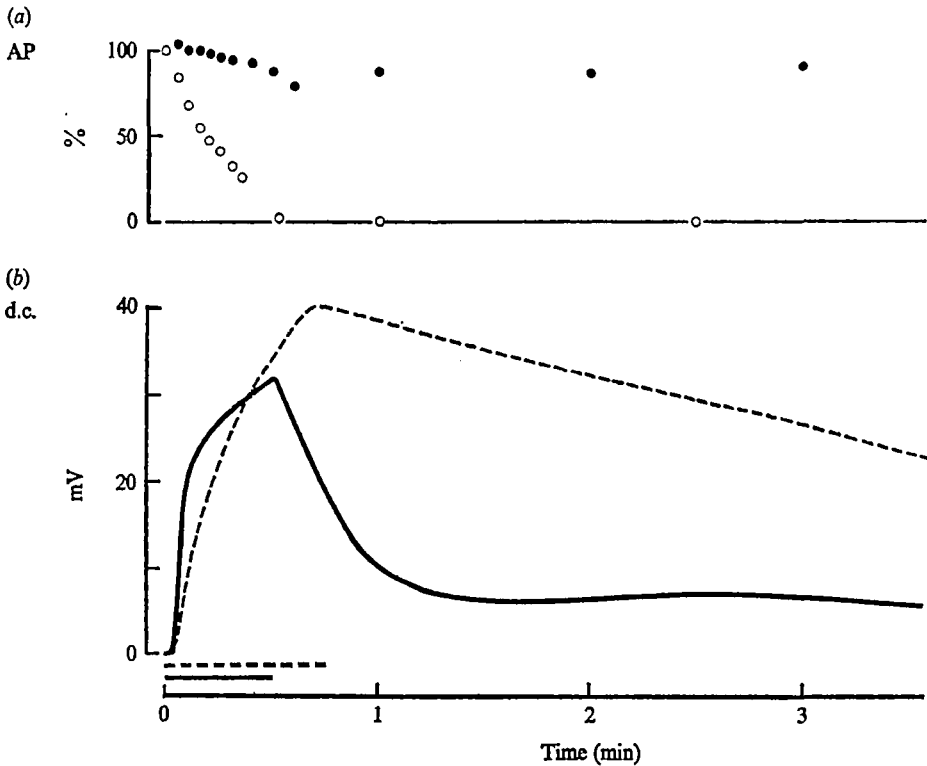


Fig. 7. Crab. Comparison of effects of isotonic KCl exposure on nerve (45 sec; open circles and dashed line) and connective (20 sec; closed circles and solid line). Sucrose gap. (a) Variation of action potential (expressed as percentage of magnitude before KCl pulse) with time. (b) Variation in d.c. potential. The time course of the d.c. changes and the relative reduction in AP amplitude on KCl exposure are clearly different in connective and nerve.

have been obtained with an intracellular microelectrode, indistinguishable from the sucrose gap record of Fig. 11(a) (see Fig. 10a, b). The shape of the potential change in Fig. 11(a), (b) is obviously not simple, and certainly contains more than one component. That recording with an extracellular microelectrode (across peripheral layers including the perineurium) gives the trace shown in Fig. 11(c) suggests this may be one component of the complex recorded in 11(a), (b). Electrodes positioned as shown in Fig. 11(a) and (b) would be expected to pick up any perineurial component, and in addition, any axon membrane depolarization. Subtraction of trace 11(c) from 11(b) or 11(a) would then be expected to leave the axon membrane component (Fig. 11d).

In Fig. 12(a) the record from Fig. 10(d) is subjected to this kind of analysis, the extracellular microelectrode trace (dashed) being subtracted from the sucrose gap trace (solid line), and the resultant (dots) plotted on the same time scale. According to the model outlined above, this last should represent axon membrane depolarization.

It will be noted that virtually the whole of the slow phase of recovery recorded in sucrose gap or with intracellular microelectrode should be due to repolarization at the axon membrane (Fig. 12a). The extent of depolarization at the beginning of this slow phase in the complex sucrose gap records should then be an indication

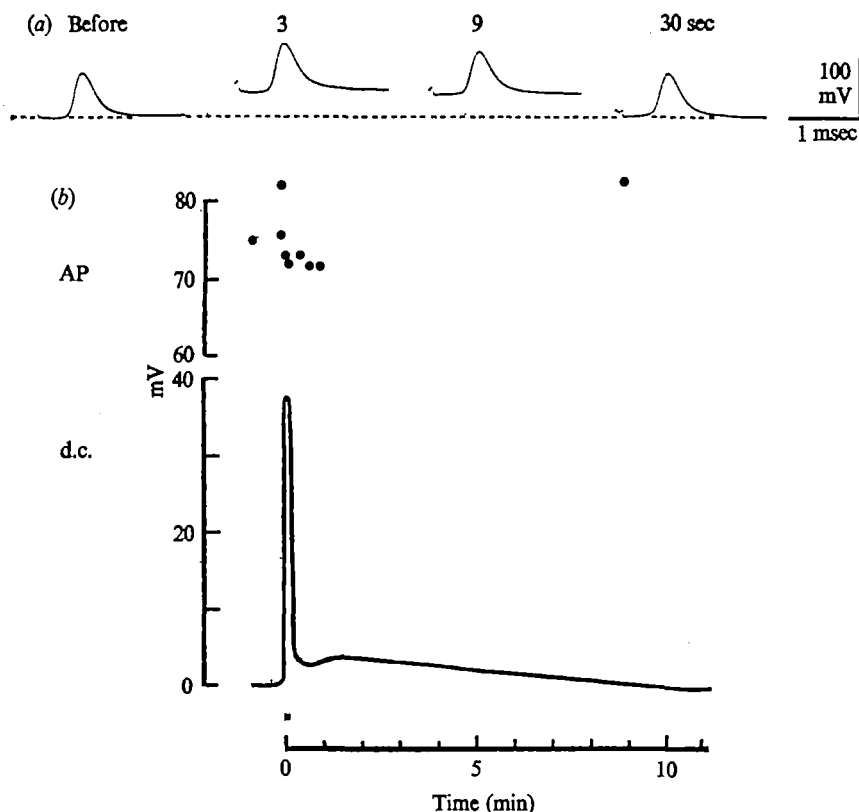


Fig. 8. Crayfish connective; 10 sec isotonic KCl. Intracellular microelectrode. (a) Action potential. (b) Variation of AP (note scale) and d.c. potential with time. There is little change in height of the AP at the time when the d.c. potential shows depolarization and repolarization by *ca.* 40 mV.

of the extent of axon membrane depolarization. Reference to the preparation illustrated in Fig. 9 shows that in this connective, where the maximum d.c. potential reached at the onset of KCl application was 35 mV, the (assumed) axon membrane depolarization never reached more than 15 mV. This is compatible with the observed reduction (not abolition) of the action potential in this preparation.

Again making use of Dalton's relation between membrane potential and bathing  $[K^+]$ , the  $[K^+]$  at the axon membrane can be calculated from the constructed axon membrane potential curve (Fig. 12a, dotted line) and plotted semilogarithmically (Fig. 12b). Simple exponentials result for depolarization and repolarization (apart from the initial phase), equivalent to potassium entry and efflux respectively, as one would expect for  $K^+$  diffusion into and out of the interstitial space. Half-times for entry and efflux from these curves are 198.97 and 9.06 min respectively (Table 1). In complex traces such as Fig. 12(a) sucrose gap trace, extrapolation of the exponential plot to the time at which elevated potassium was replaced by normal saline, should give the approximate potassium concentration at the axon surface at the end of the KCl exposure.

The model outlined above proposes that components shown in Fig. 11(c) and (d)

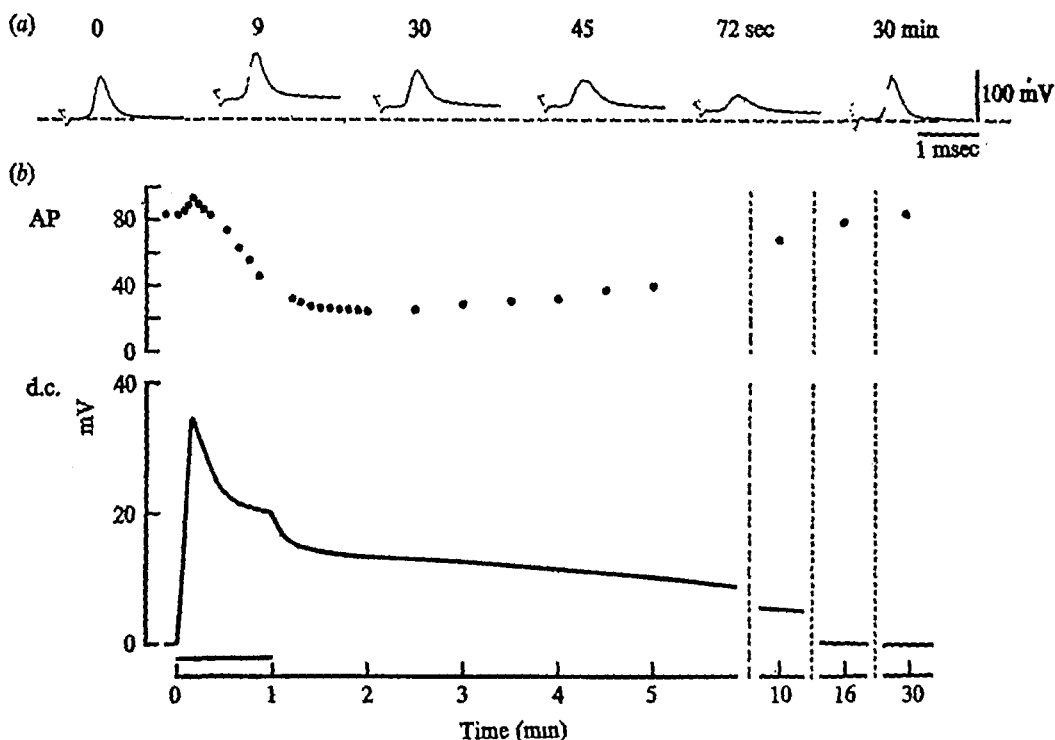


Fig. 9. Crayfish connective; 1 min isotonic KCl. Intracellular microelectrode. (a) and (b) as for Fig. 8. Note that the d.c. trace shows an initial depolarization followed by a partial repolarization in spite of maintained KCl exposure.

are summed when recording with electrode positions 11(a) or (b). It will be noted that the height of the potential  $x$  in the complex of Fig. 11(a) should be related to the height of the transient perineurial potential  $x'$  in Fig. 11(c). Potential  $y$  should be related to the extent of depolarization of the axon membrane at the end of the KCl exposure  $y'$  in 11(d), and can be used to calculate the interstitial  $[K^+]$  at this time.  $x$ , being a transient, should be independent of exposure time to KCl, while  $y$ , or the equivalent  $[K^+]$ , should increase with longer KCl exposures.

As further tests to the model, the following experiments were done.

#### *Effect of length of KCl exposure*

In a series of experiments on crayfish connective the d.c. response to different isotonic KCl exposure times was recorded. Fig. 13 shows superimposed sucrose gap traces. In this series, the height of the initial transient potential ( $x$ ) declined with successive KCl exposures, the *order* of exposure being more critical than the length of time in KCl at each exposure. In experiments where long recovery periods intervened in fresh preparations, it could be shown that the transient  $x$  was independent of KCl exposure time. A plot of transient (mV) against KCl exposure time (min) gave a regression line of  $y$  on  $x$ ,  $y = 35.29 - 0.27x$ , not significantly different from the horizontal ( $P > 0.05$ ).

From the traces of Fig. 13 it is clear that the presumed extent of axon membrane

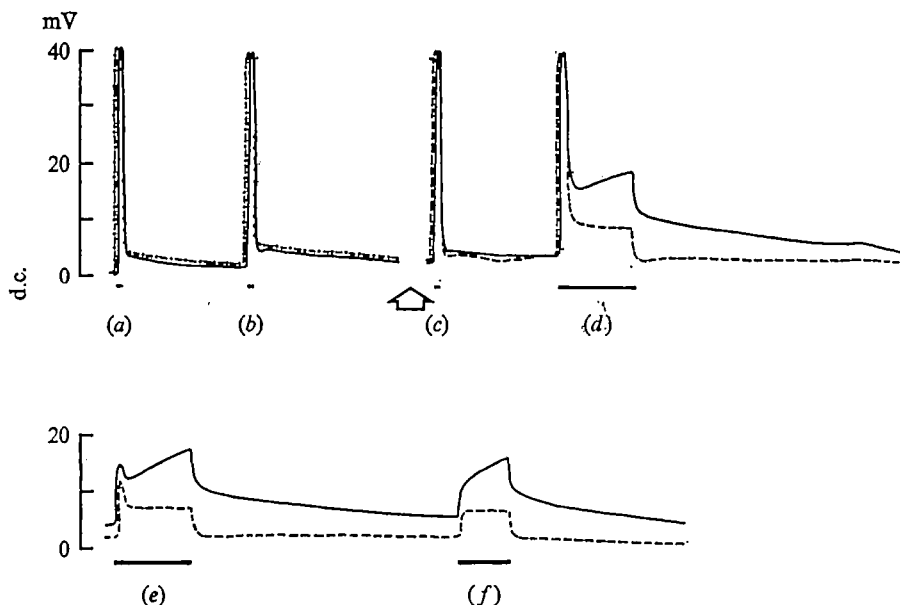


Fig. 10. Crayfish connective. D.c. response to a succession of isotonic KCl exposures, recorded by intracellular microelectrode (dashes + dots) or extracellular microelectrode (dashes), and simultaneously by sucrose gap (solid line). At broad arrow, microelectrode was withdrawn into an extracellular position. KCl exposure: (a-c), 10 sec; (d, e), 3 min; (f) 2 min.

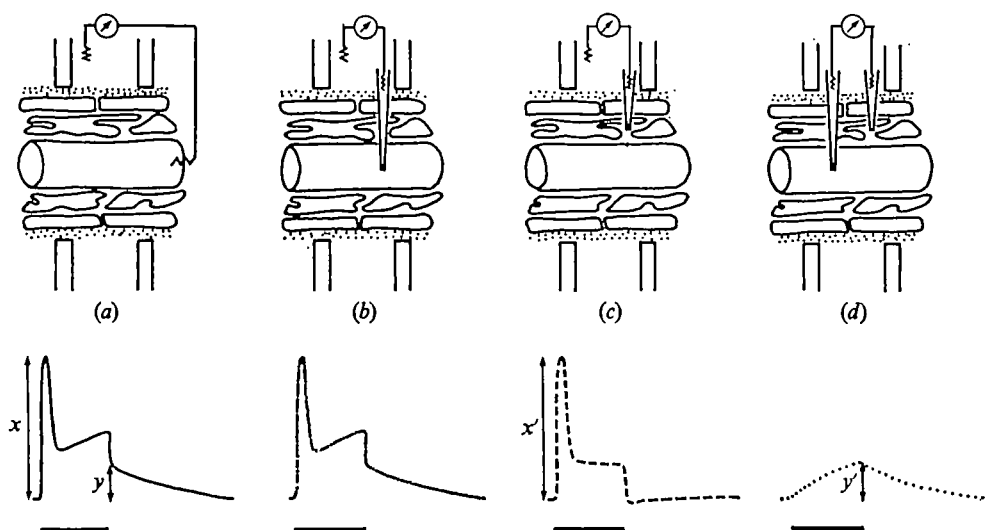


Fig. 11. Diagram showing electrode positions used (above) and d.c. records obtained (below) in the experiment of Fig. 10(d). (a) Sucrose gap, (b) intracellular microelectrode, (c) extracellular microelectrode, (d) hypothetical, record of pure axon membrane depolarization.  $x$ ,  $x'$  refer to initial transient potential;  $y$ ,  $y'$  to axon membrane depolarization at end of KCl exposure.

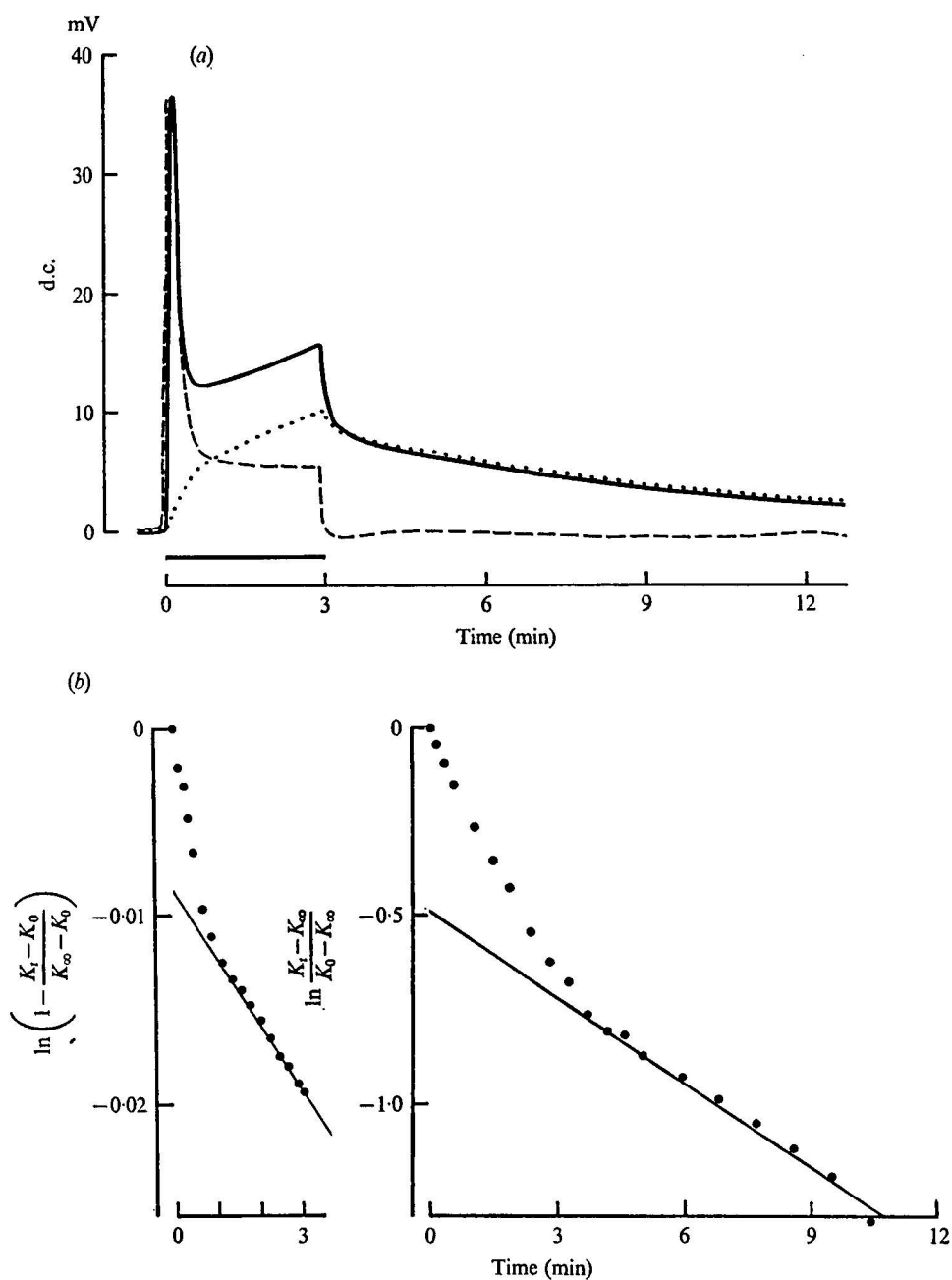


Fig. 12. (a) Analysis of d.c. record shown in Fig. 10(d). Extracellular microelectrode trace (dashed line) is subtracted from total sucrose gap trace (solid line) to yield the presumed axon membrane depolarization (dots).

(b) Semilog plot of change in  $[K^+]$  at axon surface during entry (left) and efflux (right), calculated from the dotted line of Fig. 12(a).  $T_{\frac{1}{2}}$  for entry and efflux are calculated from the slopes of the lines.



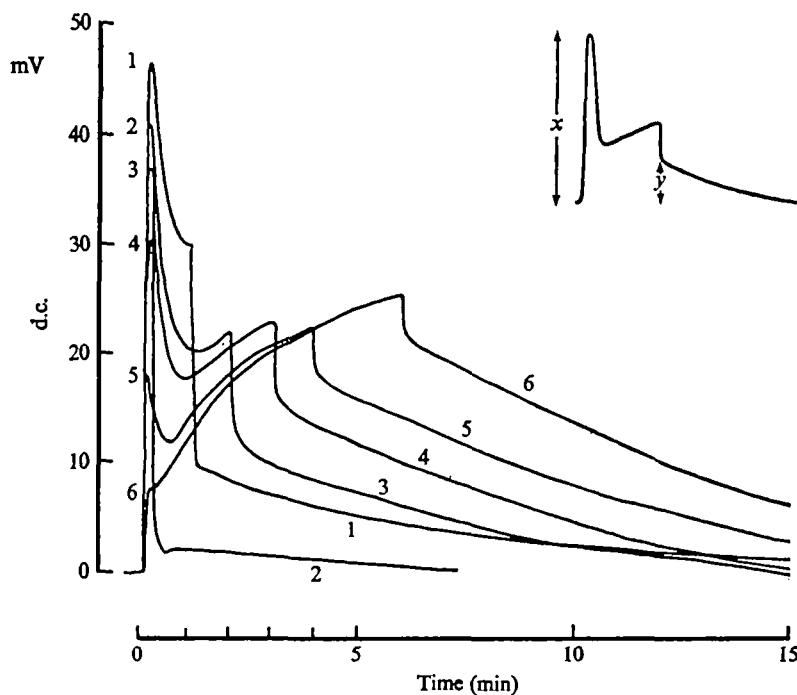


Fig. 13. Crayfish connective. Superimposed d.c. traces, sucrose gap, from a series of isotonic KCl exposures for different times. Order of exposure is indicated by numbers adjacent to each trace. The height of the transient ( $x$ ) and axon membrane depolarization ( $y$ ) can be measured from each trace; pooled data from these and similar experiments have been analysed (see text and Fig. 14).

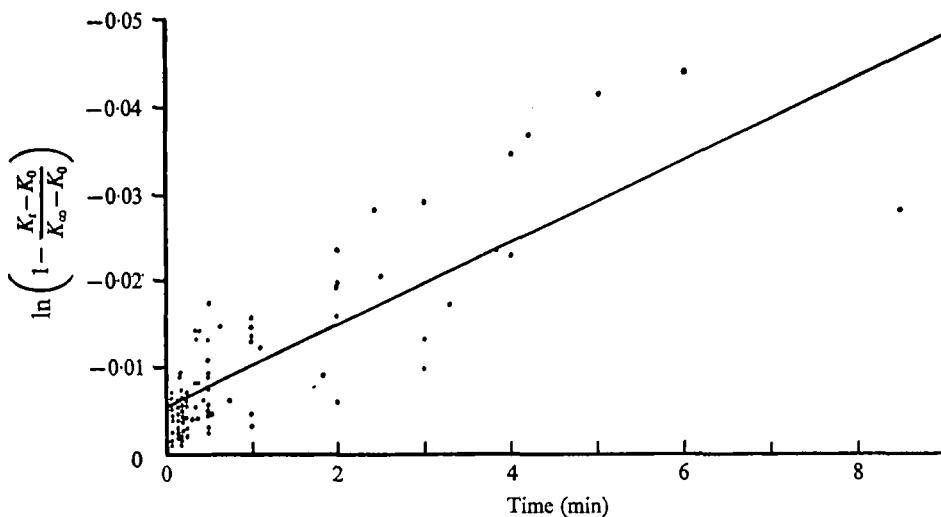


Fig. 14. Dependence of  $[K^+]$  at the axon surface on KCl exposure time. The change in  $[K^+]$  is expressed as  $\ln \left[ 1 - \frac{(K_t - K_0)}{(K_\infty - K_0)} \right]$ , and calculated from the extent of axon depolarization at the end of KCl exposure ( $y$  in Figs. 11, 13) in a series of experiments. The slope of the regression line is used to calculate the  $T_{1/2}$  for  $K^+$  entry.

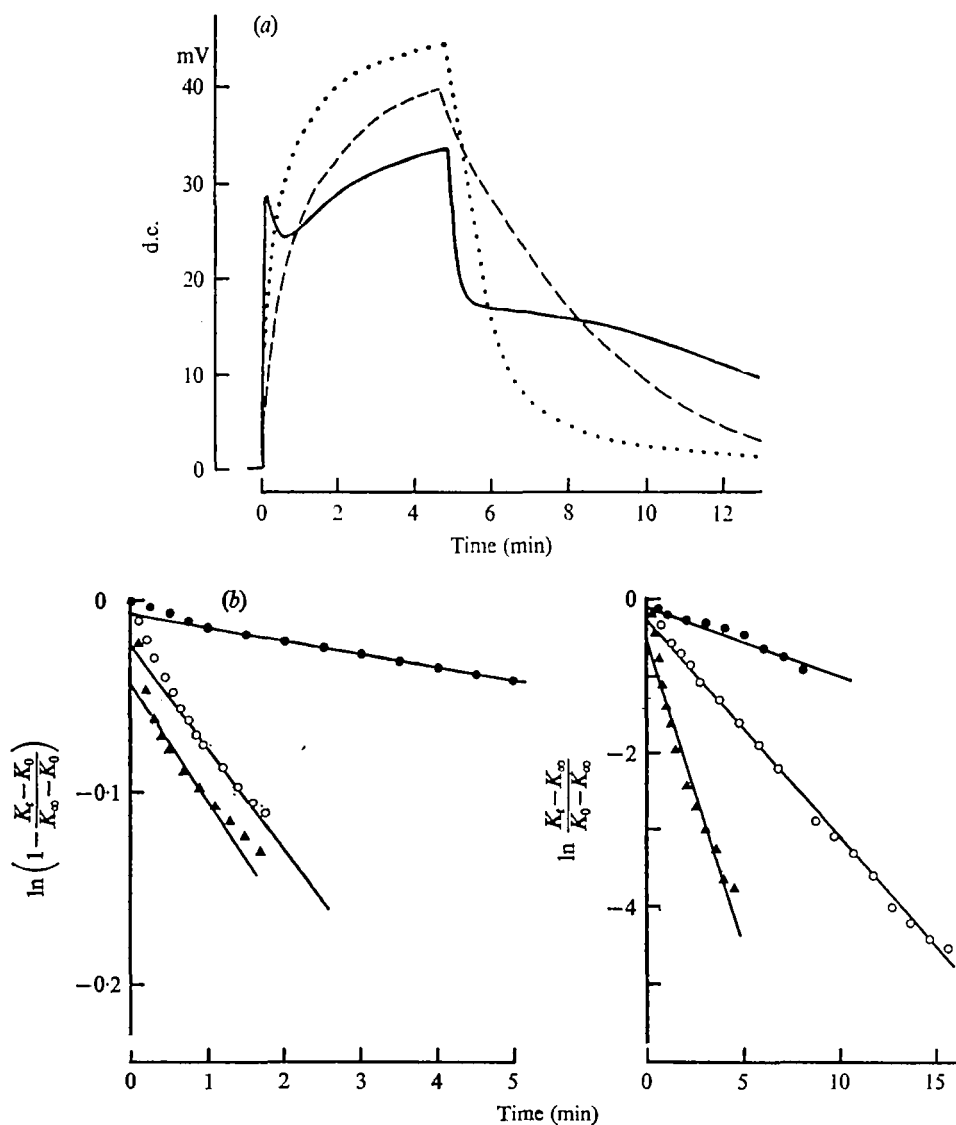


Fig. 15. (a) Comparison of d.c. response of intact and desheathed connective, and peripheral nerve, to isotonic KCl in crayfish. Solid line, intact connective; dashed line, desheathed connective; dots, peripheral nerve. Desheathing curve converts the complex d.c. trace of connective to the simpler trace characteristic of nerve.

(b) Semilog plots of change in  $[K^+]$  at axon membrane during entry (left) and efflux (right) derived from curves in (a). Solid circles, intact connective; open circles, desheathed connective; triangles, peripheral nerve. The curves for intact connective are derived by extrapolation, using the method of estimation of extent of axon depolarization outlined in text. Note that the  $[K^+]$  changes at the axon membrane occur very much faster in nerve and desheathed connective than in intact connective.

depolarization ( $y$ ) increases with exposure time. Semi-log plots of  $[K^+]$  during the slow repolarization phase have been used to calculate the interstitial  $[K^+]$  at the end of KCl exposure, for different KCl exposure times. These values are plotted in Fig. 14. For pooled experiments, the regression line of  $y$  on  $x$ , is  $y = 0.0053 + 0.0049x$ , significantly different from the horizontal ( $P < 0.001$ ). Half-time for potassium entry into the extra-axonal space of intact connectives calculated from the slope of the regression line is 142.53 min (Table 1).

The half-time for  $K^+$  efflux could be calculated from the repolarization kinetics in the same preparations (slope of plot of  $\ln [(K_t - K_\infty)/(K_0 - K_\infty)]$  *v.* time; symbols as defined in Fig. 4), and averaged 5.99 min (Table 1).

The model thus qualitatively predicts the behaviour of recognized components of the complex sucrose gap or intracellular microelectrode d.c. response to isotonic KCl.

### *Effect of desheathing connective*

The record obtained with an extracellular microelectrode in intact connective (Fig. 11*c*) shows that a transient followed by a steady-state potential is recorded across the superficial layers of the connective, the perineurium being implicated because of its organized structure. The model predicts that if the perineurium is removed by desheathing the connective, the d.c. potential change should simply reflect changes at the axon membrane (Fig. 11*d*).

Fig. 15(*a*) shows the d.c. trace obtained in a desheathed crayfish connective, superimposed on comparable traces for peripheral nerve and intact connective. The desheathing procedure converts the complex trace characteristic of intact connective, into the exponential depolarization and repolarization seen in peripheral nerve. Semi-log plots of interstitial  $[K^+]$  calculated from the potential trace, confirm the simple exponential nature of the process (Fig. 15*b*). Half-times for  $[K^+]$  entry and efflux in the desheathed preparation are 13.08 and 2.45 min respectively (Table 1) – much shorter than in intact connective, and approaching half-times for potassium fluxes in nerve.

Intermediates between the d.c. traces for intact and desheathed preparations can be obtained by different degrees of damage to the connective.

### *Model for perineurial d.c. potential change*

The desheathing experiment showed that the transient and steady-state components of connective d.c. potential are abolished by desheathing – further evidence that these components are of perineurial origin. It is helpful to construct a model of the perineurium compatible with the observed d.c. potential changes. It is assumed that adjacent perineurial cells are reasonably tightly coupled, and that bath  $[K^+]$ ,  $([K^+]_b)$  and interstitial  $[K^+]$ ,  $([K^+]_i)$  are initially similar. A sudden increase in  $[K^+]_b$  will cause a reduction of the  $[K^+]$  gradient across the outer perineurial membrane, causing a depolarization at this membrane, but because of the low permeability of junctions between perineurial cells the inner membrane will be relatively unaffected. A transient potential (the inner surface of the perineurium becoming positive with respect to the outer surface) will be set up by the asymmetrical

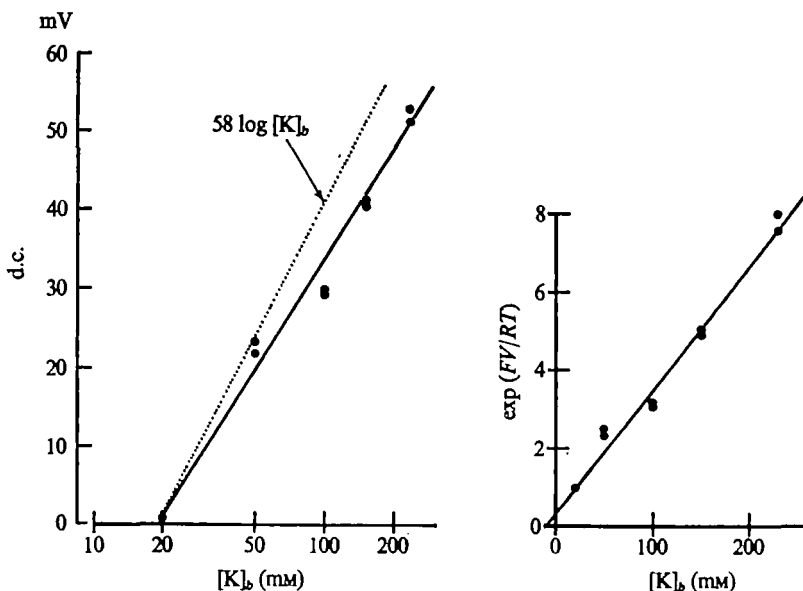


Fig. 16. Dependence of the height of the d.c. potential transient  $\pi$  (see Figs. 11, 13) on  $\log[K^+]$  in the bathing medium,  $([K^+]_b)$ . The theoretical 58 mV Nernst slope is shown for comparison. Inset: the same data, plotted in the form  $\exp(FV/RT)$  against potassium concentration, according to equation (1) of Methods.

depolarization of the perineurial layer. The initial depolarization will be transient, declining as  $K^+$  enters the interstitial space down the  $[K^+]$  gradient.

The steady-state component of the potential is more difficult to explain. It could be (a) an osmotic effect, if the perineurial junctions are more permeable to  $K^+$  than to  $Na^+$ , (b) the result of an electrogenic pump at the perineurium, (c) the consequence of a change in the selectivity of the junctions caused by elevated  $[K^+]$ , (d) due to a reservoir effect in the interstitial space so that  $[K^+]$  at the inner surface of the perineurium is kept lower than  $[K^+]_b$  for an appreciable time, (e) an artifact introduced if the extracellular electrode within the connective is some distance from the inner perineurial membrane. The experiments and analysis described so far do not enable us to distinguish between these possibilities, although the theoretical analysis of a model system (see below) suggests that a combination of hypotheses (c) and (d) may be nearest the truth.

*Effect of alterations in bathing potassium concentration  $[K^+]_b$  on the height of the transient perineurial potential*

If the initial transient is indeed due to a suddenly altered  $K^+$  gradient across the outer perineurium membrane, its amplitude should be predicted by the Nernst equation

$$E = 58 \log_{10} \frac{[K^+]_b}{[K^+]_{is}},$$

where  $[K^+]_b$  = bath  $K^+$  concentration,  $[K^+]_{is}$  = interstitial  $K^+$  concentration. If experimental conditions are such that  $[K^+]_{is}$  is constant, then the transient should

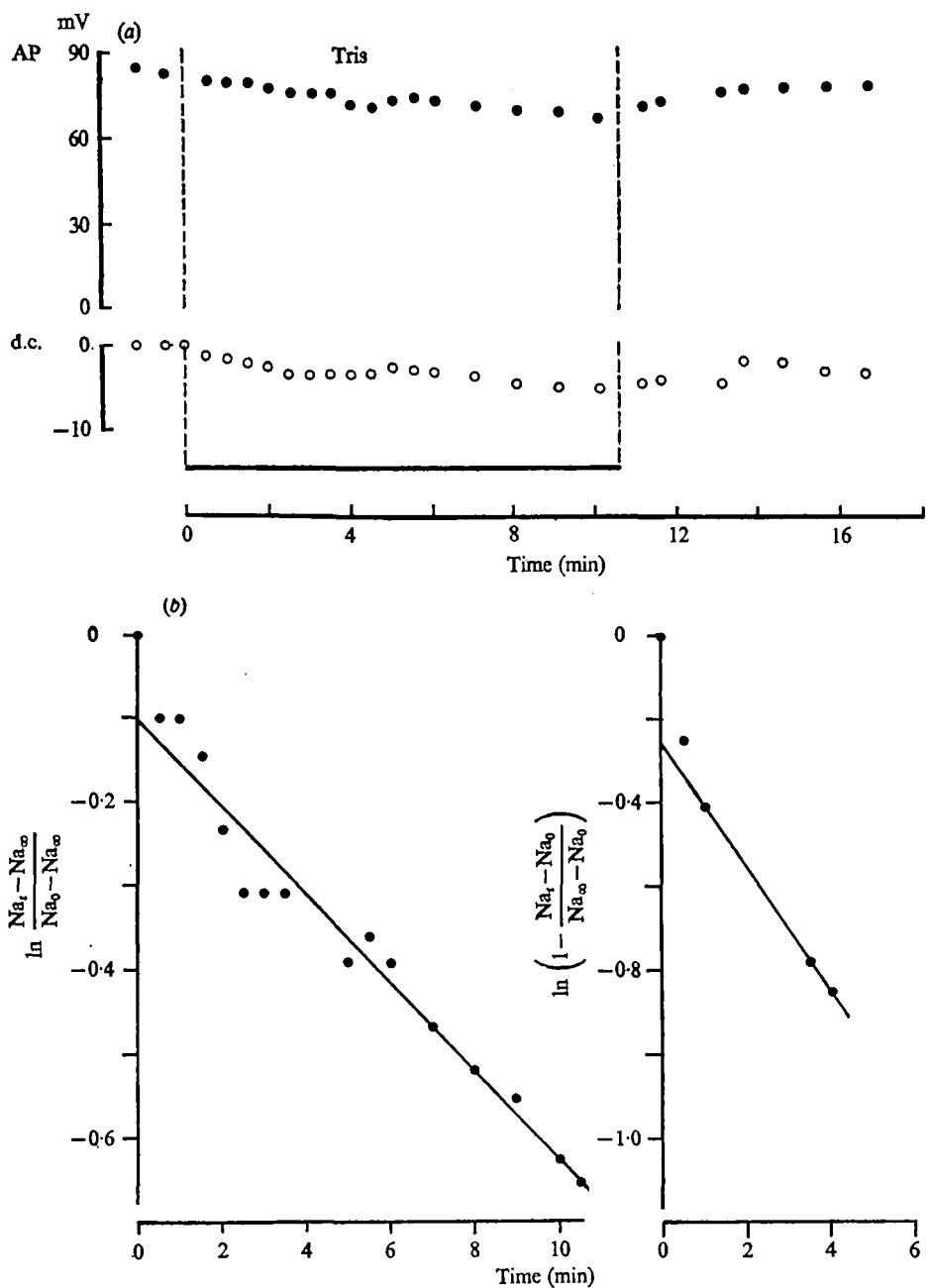


Fig. 17. (a) The effect of substituting Tris for Na<sup>+</sup> in the bathing medium on AP (solid circles) and d.c. potential (open circles) in crayfish connective; 10.5 min exposure. Intracellular microelectrode. Note that a slight hyperpolarization of the d.c. trace (downwards deflection) is observed.

(b) Changes in [Na<sup>+</sup>] at the axon surface calculated from the potential changes of (a), and plotted semilogarithmically with time, for efflux (left) and entry (right). The slope of the lines is used to calculate  $T_{\frac{1}{2}}$  for Na<sup>+</sup> efflux and uptake.

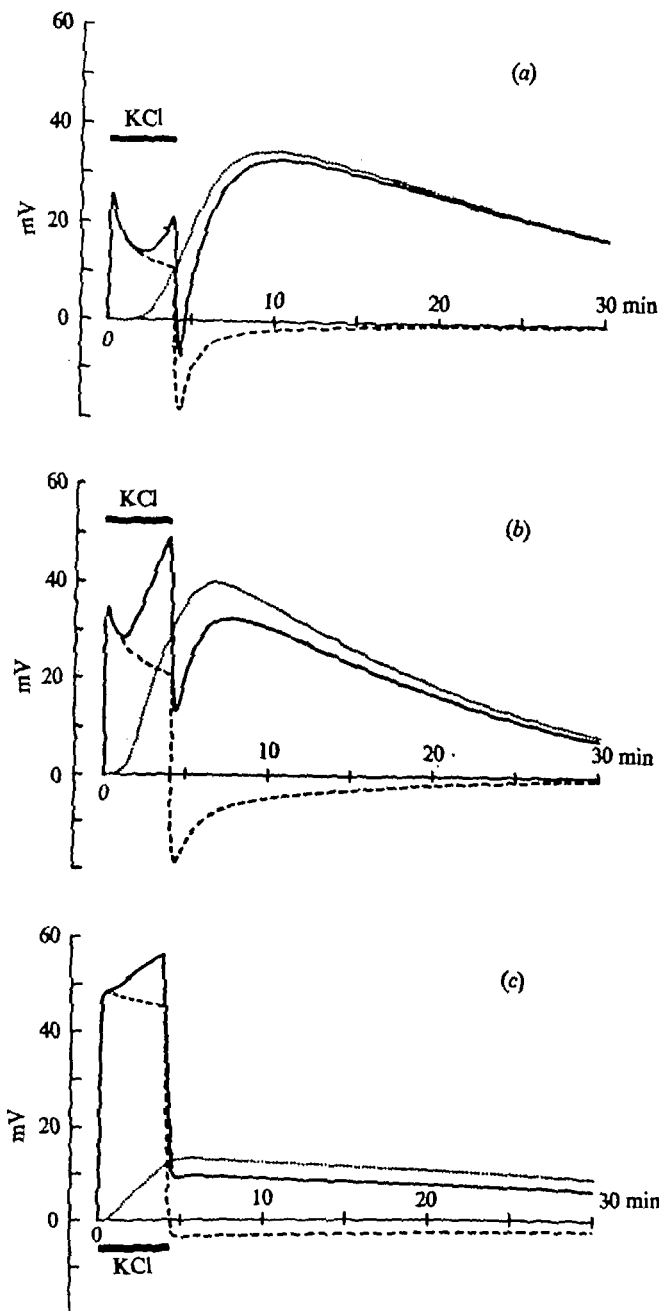


Fig. 18. Theoretical behaviour of a simple model system in response to a 4 min pulse of isotonic KCl solution, 230 mM- $K^+$  (crayfish). Three different cases are illustrated: (a) mainly diffusion-limited; (b) intermediate; (c) mainly barrier-limited. In each case the dotted line shows the axonal depolarization, the dashed curve the 'extraneuronal' or perineurial potential, and the solid line the total potential change. Parameters chosen were as follows:

	(a)	(b)	(c)
Diffusivity ( $\text{cm}^2 \text{sec}^{-1}$ ) ...	$1.0 \times 10^{-6}$	$2.5 \times 10^{-6}$	$1.0 \times 10^{-5}$
Barrier permeability* ( $\text{cm}^{-1} \text{sec}^{-1}$ )	$5.0 \times 10^{-4}$	$2.5 \times 10^{-4}$	$2.0 \times 10^{-3}$
Channel length ( $\mu\text{m}$ )	500	500	500
$A$ (see equation (1)) (mm)	30	30	30

\* Expressed per unit cross-sectional area of the diffusion channel. The absolute membrane permeability cannot, of course, be estimated until more is known about the precise location and dimensions of the extracellular pathway.

show a linear dependence on  $\log [K^+]_b$ . Fig. 16 shows the effect of different  $K^+$  concentrations on the height of the transient perineurial potential. The expected linear relation is found, with a 48 mV depolarization accompanying a 10-fold change in  $[K^+]_b$ . These observations support the model for the perineurial origin of the transient potential outlined above.

#### *Effect of substituting Tris for $Na^+$ in the bathing medium*

The experiments illustrated in Figs. 5–10, 12–15 suggest that access of  $K^+$  ions from the bathing medium to the axon surface is restricted, and Fig. 15 shows that the perineurium is at least partly responsible for this restriction. Fig. 17(a) shows the effect of substituting Tris for  $Na^+$  in the medium bathing an intact connective. As expected, the d.c. potential is little affected, although showing a slight apparent hyperpolarization. Of particular interest is the ability of the connective axons to conduct action potentials for long periods in the  $Na^+$ -free situation, although a gradual decline in the height of the action potential is observed. Stimulation at 30 Hz for 15 sec every 2 min results in a slightly more rapid decline in action potential height. It is unlikely that ions other than  $Na^+$  can carry a significant proportion of the action current in crustacean nerve (Iwasaki & Satow, 1971).

By reference to Dalton's investigation of the dependence of the height of the action potential in crayfish giant axons on bathing  $[Na^+]$ , the effective interstitial  $[Na^+]$  during and after the Tris exposure can be calculated. From the semilogarithmic plots (Fig. 17b), the half-times for  $Na^+$  movements out of and into the extra-axonal space can be calculated, averaging 9.28 and 2.91 min respectively (Table 1).

These experiments support the view that some small ions and molecules in the bathing medium have restricted access to the connective axon surface, the composition of the connective interstitial space being only slowly altered following a change in the ionic composition of the bathing medium. By contrast, conduction is more rapidly blocked in crustacean peripheral nerve bathed in  $Na^+$ -free (choline) solution (Baker, 1965a).

#### *Theoretical analysis of potassium movements in a model system*

Some representative curves calculated from the model are shown in Fig. 18. Their main features and implications will be discussed below.

### DISCUSSION

Potential changes recorded in crustacean peripheral nerve on exposure to isotonic KCl are straightforward, and can be simply interpreted as a progressive depolarization of axon membranes as  $K^+$  diffuses into the nerve interstitial space. For a simple two-compartment system (bath–interstitial space), the diffusion process should follow first-order kinetics, and as shown in Fig. 4(b), a plot of  $\ln [1 - (K_t - K_0)/(K_\infty - K_0)]$  (entry)\* or  $\ln [(K_t - K_\infty)/(K_0 - K_\infty)]$  (efflux) *v.* time gives the expected linear relationships.

\* The words 'entry' or 'access' are used here and in analogous places instead of 'uptake' to show that it is purely the change in concentration in the extracellular space adjacent to the axons which is being considered; no attempt is made to relate this to the behaviour of any 'compartment' identified by tracer measurements.

It may be concluded that the organization of peripheral nerve, in two species of crustacean, imposes little restriction on diffusion of small ions and molecules between the bathing medium or haemolymph, and nerve interstitial space. This is in agreement with previous observations (Baker, 1965*a, b*), and is compatible with the known structure of crustacean peripheral nerve, where glial layers and extracellular material would seem too loosely organized to restrict access to the interstitial space (Lane & Abbott, 1975).

The connectives of decapod central nervous system differ from peripheral nerve chiefly in the more highly organized perineurium or peripheral glial cell layer, adjacent cells of the perineurium being linked by various types of junctional complex. (Lane & Abbott, 1975). It is apparent that d.c. potentials recorded with intracellular microelectrodes or an extracellular sucrose gap technique include a potential developed across some peripheral extraneuronal layer, in addition to axon membrane depolarization. The perineurium is the most likely site of this extra component, because of its highly organized structure, forming a continuous cell layer at the periphery of the connective. It has been shown that the potential change across the perineurium when the connective is exposed to isotonic KCl can be explained as a transient potential due to the altered  $K^+$  gradient across the outwardly facing perineurium membrane, followed by a steady potential whose explanation will be discussed below. Evidence that the transient plus steady-state potential is a component of the complex d.c. potential recorded with intracellular microelectrodes and sucrose gap technique, and is moreover associated with the perineurium, includes the following:

(a) The height of the initial potential is independent of KCl exposure time, suggesting a transient potential due to a sudden change in  $K^+$  gradients.

(b) The rapidity of the transient response to KCl exposure suggests a very peripheral structure is involved.

(c) The height of the transient potential shows a linear dependence on  $\log [K^+]$  in the bathing medium, *ca.* 48 mV depolarization accompanying a 10-fold change in  $[K^+]_b$ . This suggests that a structure acting as a fairly selective  $K^+$  electrode is involved. A continuous cellular layer with a degree of close association between adjacent cells seems implicated.

(d) If a microelectrode is positioned extracellularly within the connective, it should record potential differences across peripheral layers of the connective between interstitial space and bath. Records from such a preparation include a transient and a steady-state potential difference on exposure to isotonic KCl.

(e) The transient plus steady-state component of complex d.c. potential traces, recorded with sucrose gap, disappears when the connective is desheathed. In the insect, desheathing removes the neural lamella and damages the perineurium and underlying glia (Lane & Treherne, 1970).

(f) The development of substantial potential differences across the perineurium would be expected to accompany considerable restriction of ionic movements between the extracellular spaces and the bathing medium. That this is indeed the case is shown by calculating the extent of axon membrane depolarization, by subtracting the 'perineurial' potential from the complex sucrose-gap record. This leaves a potential change compatible with a very slow diffusive access of  $K^+$  to the connective



axon membranes: half-times for potassium entry are much longer than in peripheral nerve or desheathed connectives (Table 1). Extracellularly and intracellularly recorded action potentials in connectives are only slowly affected by elevated potassium concentrations in the bathing medium, again suggesting a very restricted access of  $K^+$  to the axon membranes (Fig. 6).

(g) Movements of sodium ions are also subject to restriction, as shown by the behaviour of the action potential when intact connectives are exposed to a saline with sodium ions replaced by Tris. The degree of restriction is, however, considerably less than that of potassium uptake (Table 1): this, together with the apparent degree of asymmetry between entry and efflux of both sodium and potassium (efflux being respectively slower and faster than entry in the two cases), suggests the involvement of a specialized structure in the regulation of ionic movements. In this context, the situation may be compared with that in cockroach connectives, where a more marked asymmetry in sodium movements has been found (Schofield & Treherne, 1975).

Theoretical analysis of a simple model system lends some support to these general considerations. Fig. 18 shows some representative curves, which may be compared with the experimental traces of Fig. 10 and 12(a). The model system, consisting of a peripheral permeability barrier in series with a long diffusion channel, is able to reproduce qualitatively the transient and slow phases of the potential change in high potassium, the 'plateau' phase of the extraneuronal potential and the gradual recovery on returning to normal saline. There are, however, important differences between theory and experiment which suggest that the real situation may be considerably more complex than the model. The two principal discrepancies are in the temporal relationship between axonal depolarization and decay of the extraneuronal potential, and in the behaviour of the latter on returning to normal saline.

In the model system, as in the experiments, raising the external potassium concentration produces an 'extraneuronal' potential which is initially large but decays roughly exponentially, reaching a 'plateau' of variable height. This decay is due to a progressive build-up of potassium ions at the inner surface of the peripheral barrier, and is followed by a gradual depolarization of the axon as these ions diffuse down the connecting channel. The extraneuronal potential does not fall to zero while this diffusion is taking place, because the progressive filling-up of the extracellular system requires a continuing net inflow of potassium ions, which in turn requires the maintenance of a concentration gradient across the peripheral barrier.

Once the extraneuronal potential has decayed to a relatively low level, the concentration of potassium ions at the inner face of the barrier must have risen to a value comparable with that in the external medium. The concentration at the axon will therefore also rise, after a delay determined by diffusivity and the length of the connecting channel. The rate of depolarization of the axon is thus closely related to the rate of decay of the extraneuronal potential. This feature is illustrated by Fig. 18(a)-(c), showing a series of theoretical curves with increasing diffusivity and decreasing barrier permeability. In (a), access to the axon-surface is mainly diffusion-limited, whereas in (c) barrier permeability is the principal determining factor. Case (b) is intermediate.

The experimental results do not fit well into any of these categories: rapid decay

of the extraneuronal potential is followed by a very slowly developed axonal depolarization, half-times for potassium access being generally in excess of 100 min (Fig. 12*b* and Table 1). The time-course of the extra-axonal potassium concentration is not sigmoid, as would be expected for a long, restricted diffusion pathway (Fig. 18*a*), but occurs if anything, more rapidly during the initial part of the curve (Fig. 12*a*).

This type of behaviour could be explained in three ways: either diffusion from the peripheral barrier to the axon is severely restricted, the site of such restriction being localized, separate from the barrier across which the extraneuronal potential is measured and closer to the axon; or access to the axon is effectively hindered by the presence of a large reservoir (e.g. the glia) which must be filled before the extracellular concentration can rise; or the decay of the extraneuronal potential is due to a change occurring in the peripheral barrier itself, rather than to the simple accumulation of ions at its inner face.

The first of these possibilities cannot be eliminated, but there is no obvious structure which could form such a site of local restriction. The second barrier, if it exists, would need to have a very particular set of ionic permeabilities, since no potential difference is ever to be recorded across it.

A 'reservoir' effect of the glial cells could be created by the action of a sodium-potassium exchange pump, removing potassium ions from the extracellular spaces in exchange for intracellular sodium. If the pump is not quite able to keep pace with the influx of potassium from the external medium, then the extracellular concentration will rise gradually. However, in order to explain the observed behaviour, one must assume that the pump does not begin to operate until the extracellular potassium concentration has risen substantially; applying equation (1) of Methods to the 'plateau' phase of the extraneuronal potential in Fig. 12(*a*) shows that the extracellular potassium concentration apparently rises to about 170 mM during the first minute of exposure to isotonic KCl. It could be argued that the 'plateau' is the result of a dynamic balance between passive influx from the bathing medium and a progressively more active pump, but the effect of such a balance can be shown mathematically to be just like that of a barrier with a lower permeability: it cannot produce the observed imbalance between rates of axonal depolarization and decay of extraneuronal potential. Exchange with the glial cytoplasm almost certainly plays some part in the long-term movement of potassium ions (cf. Pichon *et al.* 1971), as evidenced by the fact that some asymmetry between inward and outward movements persists even in desheathed preparations (Table 1). It is, however, difficult to see how active transport by the glia can by itself explain the complex behaviour seen in the present experiments.

Progressive changes in the peripheral barrier during exposure to isotonic KCl solution could take the form of simple permeability changes, or of activation of an electrogenic ion pump, transporting potassium ions outwards into the bathing medium. In the former case, a decrease in the potassium permeability could cause a partial disappearance of the specific electrical response to potassium concentration gradients; in the latter, net outward transfer of positive ions by the pump could partly neutralize the potential difference set up by inward diffusion of these ions. In either case, the effect would be to reduce the extraneuronal potential without

allowing any substantial accumulation of potassium ions inside the barrier, and also to reduce the net inflow of ions below the initial rate. That the net inflow is indeed reduced in such a way is suggested by the time-course of the axonal depolarization. The access curve of Fig. 12(b) shows two distinct phases: the later, exponential phase has a half-time of 199 min, and is preceded by a faster, complex portion (the initial part of the access curve is not expected to be strictly exponential – cf. Fig. 18). The pooled data of Fig. 14 also show this feature, in that the intercept of the regression line differs significantly from zero ( $0.01 < P < 0.02$ ). The negative intercept is a reflexion of the fact that at short KCl exposure times, the apparent half-time for  $K^+$  uptake is less than during longer KCl exposures, suggesting that a permeability change takes place during KCl exposure.

Support for the idea of a permeability change is given by the experimental behaviour on returning to normal saline. If the decay of extraneuronal potential is due to a substantial accumulation of potassium inside the peripheral barrier, then returning to a lower external concentration should produce a transient reversal of the extraneuronal potential. In fact this is not seen, the most that occurs being a small deflexion of a few mV (Fig. 12a), comparable to that expected from the barrier-limited system of Fig. 18(c). On the other hand, efflux of potassium ions from the extra-axonal space occurs comparatively fast, with a half-time of about 6 min (Table 1), so that it is necessary to assume that, on returning to normal saline the barrier quite rapidly resumes its 'normal' permeability properties. That this does not lead to a reversed extraneuronal potential is due to the fact that accumulation of potassium inside the barrier was prevented by the low permeability of the barrier during exposure to isotonic KCl. The existence of an active transport mechanism provides a better explanation for such asymmetry in ionic movements, since it always operates in the same direction, regardless of concentration gradients, but it is difficult to see how it could be shut off sufficiently rapidly to prevent a transient reversal of the extraneuronal potential, at the end of each high-potassium pulse.

Thus, although the evidence so far does not enable a firm decision to be made between the various possibilities, it does seem that the existence of a peripheral barrier (e.g. tight junctions in the perineurium) with ionic permeabilities changing reversibly in response to changes in the bathing medium can provide the simplest explanation for the electrical behaviour of crustacean central nervous connectives. The precise mechanism by which the permeabilities are made to vary is not clear; osmotic changes in perineurial cells (e.g. due to uptake of  $Cl^-$ ) could be responsible. Comparison may be made with the behaviour of frog skin (Erlij & Martinez-Palomo, 1972; Rabito, Boulau & Cerejido, 1973) and cockroach connective (Treherne, Schofield & Lane, 1973) in response to osmotic and ionic stress, and with the reversible permeability increase apparently observed in peripheral nerves of *Schistocerca* (Pichon & Treherne, 1973) in response to high potassium concentrations. Since extraneuronal potentials are only observed in crustacean connectives at potassium concentrations above 20 mM (Fig. 16), it is possible that the potentials seen at higher concentrations are the effect of transient permeability increases, triggered by the high potassium concentration.

The main problem with a mechanism dependent on a limited permeability of the perineurium is the apparent scarcity of tight junctions between these cells, although

gap junctions are frequent (Lane & Abbott, 1975). The alternative is a leakier system coupled with an active ion pump. Experiments on the effects of metabolic inhibitors may elucidate the position by proving or eliminating the involvement of active transport.

It may be noted that sodium-free (Tris) saline apparently does not trigger large permeability changes, since sodium access and efflux times are similar to those for potassium efflux,\* although sodium efflux appears slightly slower than influx (Fig. 17*b*; Table 1). The asymmetry between sodium and potassium entry and efflux could alternatively be explained by a  $\text{Na}^+ - \text{K}^+$  exchange pump at the perineurium.

The differences between crustacean peripheral nerve and connective in electrical response to elevated  $\text{K}^+$  concentrations are thus adequately explained by a peripheral perineurial diffusion barrier (limited permeability, or pump) in connective. It is worth noting that the initial permeability of the crustacean perineurium must be greater than in equivalent insect systems, as an appreciable axonal depolarization accompanies all but the briefest KCl exposures (cf. Pichon *et al.* 1971).

Other differences from the insect are that large branches of insect peripheral nerve as well as connective appear to demonstrate perineurial restriction, and that the initial height of the perineurial potential in insect connective is maintained for several minutes of KCl exposure, instead of being a transient lasting only a few seconds as in the Crustacea.

The question of the physiological significance of the crustacean observations is more difficult. It is clear that the peripheral nerve in the two decapods studied is less protected than central nervous system connective, in the sense that axons are more rapidly affected by changes in bathing medium or haemolymph composition. The fact that the perineurial barrier, while not absolute, does permit a more gradual change in brain interstitial space composition following a step change in the bathing medium could possibly allow a greater homeostasis of the internal environment of the CNS than of peripheral nerve. Thus restricted access at the perineurium would mean a greater opportunity for active mechanisms to regulate CNS interstitial fluid composition, a situation analogous to the vertebrate blood-brain barrier (Davson, 1967). There are good reasons for requiring homeostasis centrally, where synaptic integration occurs, while peripheral nerve, concerned with all-or-none events, may be less vulnerable.

It must be borne in mind, however, that the results presented here may have little relevance for normal exchanges of materials between blood and brain. The CNS of decapod Crustacea has been shown to contain an elaborate system of blood channels (Sandeman, 1967; Abbott, 1970, 1971*b*), blood entering cerebral and thoracic ganglia and connective through channels bounded by glial cells and their basement membrane. These channels open periodically at the ganglion surface, where their contents mix with haemocoel blood (Fig. 19). Under these circumstances, the main exchange pathway between blood and brain would be expected to be across these internal channel walls, the superficial layers, including the perineurium, being of less importance. An impermeability of the superficial perineurium might be a secondary

\* Note that this statement is not incompatible with the barrier having a specific potassium permeability; potassium ions can only enter the system as fast as sodium ions can escape, so that the determining factor is really  $P_{\text{Na}}$  – hence the factor  $A$  in equation (2) of Methods.

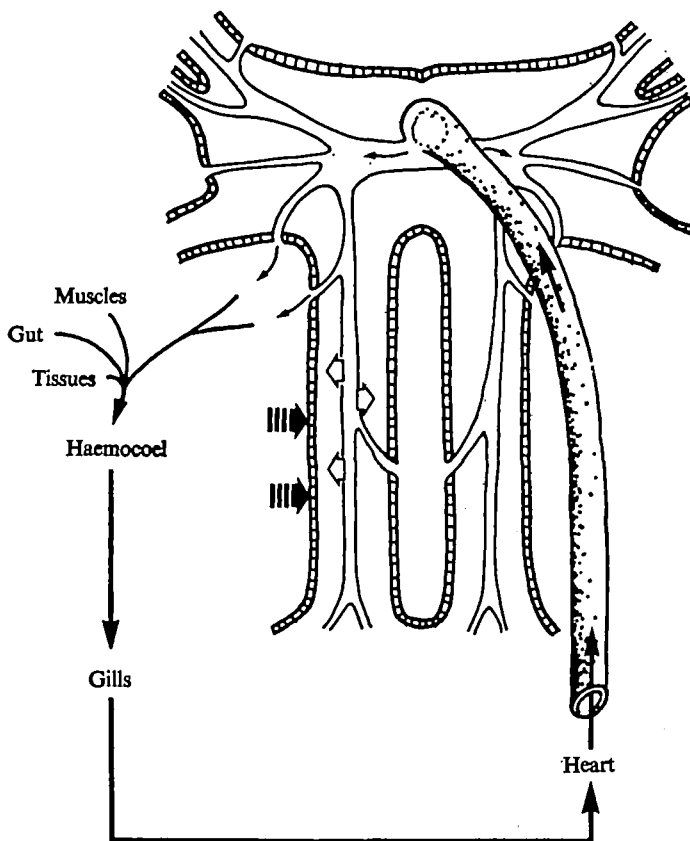


Fig. 19. Diagram of circulation in decapod brain and connective. Blood flow is probably mainly unidirectional in the animal (thin arrows) entering the CNS via the dorsal aorta, and flowing back to the heart via haemocoel and gills. Studies with isotopic and electron-dense tracers show that access to the neurones from the internal blood channels is relatively unrestricted (open arrows), while the present study has shown restriction to  $K^+$  entry across the outer surface of the connective (filled arrows).

consequence of specialization for some other function, e.g. mechanical, in resisting deformation of the central nervous system. In investigating the crustacean perineurium we might then be looking at the invertebrate equivalent of the vertebrate *dura mater*. The present study may tell us little about the permeability of the normal diffusion path between blood and brain.

An alternative possibility is that the relative impermeability of the crustacean perineurium is a specialization of physiological significance. Isotope and electron microscope tracer studies in crab cerebral ganglion have suggested that the intracerebral blood channel walls are relatively permeable to small ions, and do not form an absolute barrier even to molecules the size of ferritin (100 Å diameter; Abbott, 1972). The position occupied by the brain in *Carcinus* and *Procambarus* circulatory systems is shown in Fig. 19. A barrier between haemocoel blood and brain, but not between intracerebral blood and brain, would serve the purpose of preventing back flux of metabolic products and excretory wastes from the haemocoel pool, while permitting rapid exchange of substances with the relatively

uncontaminated blood arriving from the heart. It is interesting that in amphibian nerve the outer perineurium appears to present a greater barrier to diffusion than does the capillary lining (Krnjević, 1954).

Thus, while there appears to be considerable evidence for restricted permeability at the perineurial glial layer surrounding the central nervous system in two species of Crustacea, the present observations do not permit us to say whether this represents a barrier specialization of the perineurium, or is merely a secondary consequence of some other function (e.g. mechanical). Furthermore, while the superficial blood-brain interface appears to show reduced permeability compared with the blood-nerve interface, this need not necessarily apply also to the blood-brain interface of intracerebral blood channels. Further experiments are required to clarify this issue.

We are grateful to the Royal Society for a travel grant and to the Science Research Council for a research grant to N. J. A. Dr J. Bruner generously loaned some of the equipment used in the early studies. The drawings of fine structure are based on electron micrographs kindly provided by Dr N. J. Lane.

#### REFERENCES

- ABBOTT, N. J. (1970). Absence of blood-brain barrier in a crustacean, *Carcinus maenas* L. *Nature, Lond.* **225**, 291-3.
- ABBOTT, N. J. (1971*a*). The organization of the cerebral ganglion in the shore crab, *Carcinus maenas*. I. Morphology. *Z. Zellforsch. mikrosk. Anat.* **120**, 386-400.
- ABBOTT, N. J. (1971*b*). The organization of the cerebral ganglion in the shore crab, *Carcinus maenas*. II. The relation of intracerebral blood vessels to other brain elements. *Z. Zellforsch. mikrosk. Anat.* **120**, 410-19.
- ABBOTT, N. J. (1972). Access of ferritin to the interstitial space of *Carcinus* brain from intracerebral blood vessels. *Tissue & Cell* **4**, 99-104.
- ABBOTT, N. J. & PICHON, Y. (1973). Ionic permeability of perineurial sheath of crayfish central nervous system. *J. Physiol., Lond.* **234**, 54-6P.
- BAKER, P. F. (1965*a*). Phosphorus metabolism of intact crab nerve and its relation to the active transport of ions. *J. Physiol., Lond.* **180**, 383-423.
- BAKER, P. F. (1965*b*). A method for location of extracellular space in crab nerve. *J. Physiol., Lond.* **180**, 439-47.
- DALTON, J. C. (1958). Effects of external ions on membrane potentials of a lobster giant axon. *J. gen. Physiol.* **41**, 529-42.
- DALTON, J. C. (1959). Effects of external ions on membrane potentials of a crayfish giant axon. *J. gen. Physiol.* **42**, 971-82.
- DAVSON, H. (1967). *Physiology of the Cerebrospinal Fluid*. London: Churchill.
- ERLIJ, D. & MARTINEZ-PALOMO, A. (1972). Opening of tight junctions in frog skin by hypertonic urea solutions. *J. Memb. Biol.* **9**, 229-40.
- EVANS, P. D. (1973). The uptake of L-glutamate by the peripheral nerves of the crab *Carcinus maenas* L. *Biochim. biophys. Acta* **311**, 302-13.
- GOLDMAN, D. E. (1943). Potential, impedance and rectification in membranes. *J. gen. Physiol.* **27**, 37-60.
- VAN HARREVELD, A. (1936). A physiological solution for fresh water crustaceans. *Proc. Soc. exp. Biol. Med.* **34**, 428-32.
- IWASAKI, S. & SATOW, Y. (1971). Sodium- and calcium-dependent spike potentials in the secretory neuron soma of the X-organ of the crayfish. *J. gen. Physiol.* **57**, 216-38.
- KEYNES, R. D. & LEWIS, P. R. (1951). The resting exchange of radioactive potassium in crab nerve. *J. Physiol., Lond.* **113**, 73-98.
- KRISTENSSON, K., STRÖMBERG, E., ELOFSSON, R. & OLSSON, Y. (1972). Distribution of protein tracers in the nervous system of the crayfish (*Astacus astacus* Linné) following systemic and local application. *J. Neurocytol.* **1**, 35-47.
- KRNJEVIĆ, K. (1954). Some observations on perfused frog sciatic nerves. *J. Physiol., Lond.* **123**, 338-56.

- LANE, N. J. & ABBOTT, N. J. (1975). The organization of the nervous system in the crayfish *Procambarus clarkii*, with emphasis on the blood-brain interface. *Cell & Tiss. Res.* (in the Press).
- LANE, N. J. & TREHERNE, J. E. (1970). Uptake of peroxidase by the cockroach central nervous system. *Tissue & Cell* **2**, 413-25.
- LANE, N. J. & TREHERNE, J. E. (1972). Studies on perineurial junctional complexes and the sites of uptake of microperoxidase and lanthanum by the cockroach central nervous system. *Tissue & Cell* **4**, 427-36.
- LANE, N. J. & TREHERNE, J. E. (1973). The ultrastructural organization of peripheral nerves in two insect species (*Periplaneta americana* and *Schistocerca gregaria*). *Tissue & Cell* **5**, 703-14.
- PANTIN, C. F. A. (1946). *Notes on Microscopical Techniques for Zoologists*. Cambridge: University Press.
- PICHON, Y., MORETON, R. B. & TREHERNE, J. E. (1971). A quantitative study of the ionic basis of extraneuronal potential changes in the central nervous system of the cockroach (*Periplaneta americana* L.). *J. exp. Biol.* **54**, 757-77.
- PICHON, Y. & TREHERNE, J. E. (1970). Extraneuronal potentials and potassium depolarization in cockroach giant axons. *J. exp. Biol.* **53**, 485-93.
- PICHON, Y. & TREHERNE, J. E. (1973). An electrophysiological study of the sodium and potassium permeabilities of insect peripheral nerves. *J. exp. Biol.* **59**, 447-61.
- PROSSER, C. L. (1940a). Effects of salts upon 'spontaneous' activity in the nervous system of the crayfish. *J. cell. comp. Physiol.* **15**, 55-65.
- PROSSER, C. L. (1940b). Action potentials in the nervous system of the crayfish. Effects of drugs and salts upon synaptic transmission. *J. cell. comp. Physiol.* **16**, 25-38.
- PROSSER, C. L. (1943). An analysis of the action of salts upon abdominal ganglia of crayfish. *J. cell. comp. Physiol.* **22**, 131-45.
- RABITO, C. A., BOULAN, E. R. & CEREIJIDO, M. (1973). Effect of the composition of the inner bathing solution on transport properties of the frog skin. *Biochim. biophys. Acta* **311**, 630-9.
- ROEDER, K. D. (1941). The effect of potassium and calcium on the spontaneous activity of the isolated crayfish nerve cord. *J. cell. comp. Physiol.* **18**, 1-9.
- SANDEMAN, D. C. (1967). The vascular circulation in the brain, optic lobes and thoracic ganglia of the crab *Carcinus*. *Proc. R. Soc. B*, **168**, 82-90.
- SCHOFIELD, P. K. & TREHERNE, J. E. (1975). Sodium transport and lithium movements across the insect blood-brain barrier. *Nature, Lond.* **255**, 723-5.
- SHIVERS, R. R. (1970). Fine structure of crayfish optic ganglia vascularization and permeability. *J. Cell Biol.* **47**, 191a.
- STÄMPFLI, R. (1954). A new method for measuring membrane potentials with external electrodes. *Experientia* **10**, 508-9.
- TREHERNE, J. E., LANE, N. J., MORETON, R. B. & PICHON, Y. (1970). A quantitative study of potassium movements in the central nervous system of *Periplaneta americana*. *J. exp. Biol.* **53**, 109-36.
- TREHERNE, J. E., SCHOFIELD, P. K. & LANE, N. J. (1973). Experimental disruption of the blood-brain barrier system in an insect (*Periplaneta americana*). *J. exp. Biol.* **59**, 711-23.